

## RESEARCH ARTICLE

# Review of technology specific degradation in crystalline silicon, cadmium telluride, copper indium gallium selenide, dye sensitised, organic and perovskite solar cells in photovoltaic modules: Understanding how reliability improvements in mature technologies can enhance emerging technologies

Jeff Kettle<sup>1</sup>  | Mohammadreza Aghaei<sup>2,3</sup>  | Shahzada Ahmad<sup>4,5</sup> | Andrew Fairbrother<sup>6</sup>  | Stuart Irvine<sup>7</sup>  | Jesper J. Jacobsson<sup>8</sup> | Samrana Kazim<sup>4,5</sup> | Vaidotas Kazukauskas<sup>9</sup> | Dan Lamb<sup>7</sup>  | Killian Lobato<sup>10</sup>  | Georgios A. Mousdis<sup>11</sup>  | Gernot Oreski<sup>12</sup>  | Angele Reinders<sup>13,14</sup>  | Jurriaan Schmitz<sup>14</sup>  | Pelin Yilmaz<sup>14,15</sup> | Mirjam J. Theelen<sup>15</sup> 

<sup>1</sup>James Watt School of Engineering, University of Glasgow, Glasgow, UK

<sup>2</sup>Department of Ocean Operations and Civil Engineering, Norwegian University of Science and Technology (NTNU), Alesund, Norway

<sup>3</sup>Energy Technology Group, Department of Mechanical Engineering, Eindhoven University of Technology, Eindhoven, the Netherlands

<sup>4</sup>BCMaterials, Basque Center for Materials, Applications and Nanostructures, UPV/EHU Science Park, Leioa, Spain

<sup>5</sup>IKERBASQUE, Basque Foundation for Science, Bilbao, Spain

<sup>6</sup>Photovoltaics ThinFilm Electronics Laboratory, École Polytechnique Fédérale de Lausanne (EPFL), Institute of Microengineering (IMT), Neuchâtel, Switzerland

<sup>7</sup>Centre for Solar Energy Research, College of Engineering, Swansea University, St. Asaph, UK

<sup>8</sup>Institute of Photoelectronic Thin Film Devices and Technology, Key Laboratory of Photoelectronic Thin Film Devices and Technology of Tianjin, College of Electronic Information and Optical Engineering, Nankai University, Tianjin, China

<sup>9</sup>Institute of Photonics and Nanotechnologies, Vilnius University, Vilnius, Lithuania

<sup>10</sup>Instituto Dom Luiz, Faculdade de Ciências, Universidade de Lisboa, Lisboa, Portugal

<sup>11</sup>National Hellenic Research Foundation, Theoretical and Physical Chemistry Institute, Athens, Greece

<sup>12</sup>Polymer Competence Center Leoben GmbH, Leoben, Austria

<sup>13</sup>Energy Technology and Fluid Dynamics Group, Eindhoven University of Technology, Eindhoven, The Netherlands

<sup>14</sup>MESA+ Institute for Nanotechnology, University of Twente, Enschede, The Netherlands

<sup>15</sup>TNO partner in Solliance, Eindhoven, The Netherlands

## Correspondence

Jeff Kettle, James Watt School of Engineering, University of Glasgow, Glasgow, UK.  
Email: [jeff.kettle@glasgow.ac.uk](mailto:jeff.kettle@glasgow.ac.uk)

## Abstract

A comprehensive understanding of failure modes of solar photovoltaic (PV) modules is key to extending their operational lifetime in the field. In this review, first, specific

**Abbreviations:** Al-BSF, aluminium back surface field [solar cell]; ALT, accelerated life testing; a-Si, amorphous silicon; BoS, balance of system; CdS, cadmium sulphide; CdTe, cadmium telluride; CIGS, copper indium gallium selenide; c-Si, crystalline silicon; EL, electroluminescence; EVA, ethylene-vinyl acetate; FA, formamidineum; FF, fill factor; HTM, hole transporting materials; IBC, interdigitated back contact (solar cell); IR, infrared; ITO, indium tin oxide; LCA, life cycle assessment; LETID, light and elevated temperature induced degradation; LID, light induced degradation; MA, methyl ammonium; MHP, metal halide perovskite (solar cell); MPPT, maximum power point tracking; NFA, non-fullerene acceptors; OPV, organic photovoltaic; PCE, power conversion efficiency; PERC, passivated emitter and rear contact (solar cell); PID, potential induced degradation; PV, photovoltaic; RH, relative humidity; SHJ, silicon heterojunction (solar cell); TCO, transparent conducting oxide; TOPCon, tunnel oxide passivated contacts (solar cell); UV, ultraviolet; Voc, open-circuit voltage.

This is an open access article under the terms of the [Creative Commons Attribution](https://creativecommons.org/licenses/by/4.0/) License, which permits use, distribution and reproduction in any medium, provided the original work is properly cited.

© 2022 The Authors. Progress in Photovoltaics: Research and Applications published by John Wiley & Sons Ltd.

**Funding information**

European Cooperation in Science and Technology

failure modes associated with mature PV technologies, such as crystalline silicon (c-Si), copper indium gallium selenide (CIGS) and cadmium telluride (CdTe), are framed by sources of specific failure modes, their development from the early-developmental stages onwards and their impact upon long term performance of PV modules. These failure modes are sorted by both PV technology and location of occurrence in PV modules, such as substrate, encapsulant, front and rear electrode, absorber and inter-layers. The second part of the review is focused on emerging PV technologies, such as perovskites solar cells, dye sensitised and organic PVs, where due to their low to medium technology readiness levels, specific long-term degradation mechanisms have not fully emerged, and most mechanisms are only partially understood. However, an in-depth summary of the known stability challenges associated with each emerging PV technology is presented. Finally, in this paper, lessons learned from mature PV technologies are reviewed, and considerations are given in to how these might be applied to the further development of emerging technologies. Namely, any emerging PV technology must eventually pass industry-standard qualification tests, while warranties for the lifetime of modern c-Si-based modules might be extended beyond the existing warranted life of 25 years.

**KEYWORDS**

climate, degradation, energy payback time, photovoltaics, reliability, solar cells, solar photovoltaic modules, stress, wear-out

## 1 | INTRODUCTION

The degradation of photovoltaic (PV) modules is one of the key factors that influences the cost of the electricity produced over their warranted life time of 25 years,<sup>1,2</sup> while several PV manufacturers are now estimating a useful life of more than 40 years.<sup>3</sup> To reduce the degradation, it is hence imperative to know the degradation and failure phenomena. During their operational lifetime, PV modules are subjected to numerous environmental stresses such as light, heat, moisture and mechanical stress, which are largely responsible for these phenomena.<sup>4</sup> To optimise reliability and predictability, and to enhance the module lifetime, it is crucial that degradation and failure mechanisms are known and can be easily recognised and contained.

This review article provides a comprehensive review of degradation and failure phenomena in existing mature and new emerging PV technologies. For this review, literature originating from the past 30 years has been explored by a team of 16 PV experts from various organisations who are members of Working Group 2 on Reliability and Durability of PV of COST Action PEARL PV in the period from September 2018 until July 2021. A first review paper of the expert group, which was published in the beginning of 2022, dealt with reliability metrics, provided a summary of the main stress factors and how they influence module degradation and gave a detailed review of degradation and failure modes.<sup>5</sup>

Failure modes are different between differing technologies due to material and process challenges, as shown in Table 1. As a result, this

review has been partitioned into three sections. The first part focuses on the technology specific degradation modes of mature PV technologies and introduces degradation modes found in silicon PV (Section 2.1), cadmium telluride (CdTe) (Section 2.2) and copper indium gallium selenide (CIGS) (Section 2.3). In the second part, a review of known failure modes and areas of future research for emerging technologies such as dye sensitised solar cells (DSCs) (Section 3.2), organic PV (OPV) (Section 3.3) and perovskite solar cells (MHP) (Sections 3.4) is enclosed. Section 3 is focused upon improving the intrinsic stability of emerging technologies, as these technologies do not possess the same types of defects seen in mature technologies. In the final part, it is discussed how known failure mechanisms and developmental issues that were discovered in mature and commercially available PV technologies might be applied to emerging PV technologies. The long-term stability of third generation PV technologies, such as perovskite PV, remains a challenge and needs to be addressed for rapid commercialisation. This paper works on the hypothesis that learning lessons from mature technologies might speed up development in reliability of these emerging technologies.

## 2 | DEGRADATION AND FAILURE OF MASS-PRODUCED TECHNOLOGIES

Even though different types of environmental, electrical and mechanical stress factors are common to all PV technologies, responses of

**TABLE 1** Summary of the specific degradation and failure mechanisms of the PV technologies discussed in this article (schematics of technologies are given in Figure 1)

	Substrate, front glass or backsheet	Encapsulant	Front (f) and rear (r) electrode	Absorber (A) and interlayers (I)
c-Si	<ul style="list-style-type: none"> <li>• Backsheet cracking and delamination</li> </ul>	<ul style="list-style-type: none"> <li>• Burn marks</li> </ul>	<ul style="list-style-type: none"> <li>• Snail trails (f)</li> <li>• Solder bond and ribbon failures (f, r)</li> </ul>	<ul style="list-style-type: none"> <li>• Cell cracks (A)</li> <li>• Hot spots (A)</li> <li>• PID, LID, LETID (A)</li> </ul>
CdTe		<ul style="list-style-type: none"> <li>• Edge sealant failure</li> </ul>	<ul style="list-style-type: none"> <li>• PID (f)</li> <li>• Cu diffusion to front Junction (r)</li> <li>• Molybdenum back contact oxidation (r)</li> </ul>	<ul style="list-style-type: none"> <li>• Recombination centres due to sodium (glass migration) (A)</li> </ul>
CIGS		<ul style="list-style-type: none"> <li>• Edge sealant failure</li> </ul>	<ul style="list-style-type: none"> <li>• Increase of ZnO:Al resistivity (f)</li> <li>• PID (f)</li> <li>• Molybdenum back contact oxidation (r)</li> </ul>	<ul style="list-style-type: none"> <li>• PID (A)</li> <li>• Alkali accumulation at the ZnO:Al and pn junction (I)</li> <li>• Wormlike defect formation (A)</li> </ul>
DSC	<ul style="list-style-type: none"> <li>• Pin holes in (flexible) barrier films</li> </ul>	<ul style="list-style-type: none"> <li>• Incompatibility of encapsulant with electrolyte</li> <li>• Edge sealant failure</li> </ul>	<ul style="list-style-type: none"> <li>• Dissolution of active later into electrolyte (r).</li> <li>• Change of electrocatalytic properties (r)</li> <li>• Dissolution from the substrate (r)</li> </ul>	<ul style="list-style-type: none"> <li>• Dye molecule photodegradation (A)</li> <li>• Electrolyte photodegradation (A)</li> <li>• Reactions between the dye and electrolyte (A)</li> <li>• Oxidation and reduction reactions at the TiO<sub>2</sub> surface (A)</li> </ul>
OPV	<ul style="list-style-type: none"> <li>• Pin holes in (flexible) barrier films</li> </ul>	<ul style="list-style-type: none"> <li>• Edge sealant failure</li> </ul>	<ul style="list-style-type: none"> <li>• Chemical degradation or oxidation of electrode (f, r)</li> <li>• Electrode diffusion (f, r)</li> <li>• Electrode cracking (f, r)</li> <li>• Electrode delamination (f, r)</li> </ul>	<ul style="list-style-type: none"> <li>• Chemical or photo degradation of the electron donor/acceptor (A)</li> <li>• Loss of percolating paths due to blend reorganisation (A)</li> <li>• Change in energy levels (A, I)</li> <li>• Metastable film morphology (A)</li> <li>• Hole/Electron transport layer diffusion or decomposition (I)</li> <li>• Degradation of the quality of the absorber and electrode interface (I)</li> </ul>
MHP	<ul style="list-style-type: none"> <li>• Information not available</li> </ul>	<ul style="list-style-type: none"> <li>• Information not available</li> </ul>	<ul style="list-style-type: none"> <li>• Au or Ag corrosion due to iodine migration (r)</li> <li>• Electrode diffusion into charge selective layers (r).</li> <li>• Oxide formation leading to unfavourable interface with charge selective layers (r)</li> </ul>	<ul style="list-style-type: none"> <li>• Loss of absorption due to absorber layer degradation (intrinsic, moisture or photoinduced) (A)</li> <li>• Migration of dopant from interlayer to absorber layer (A)</li> <li>• Phase separation (A)</li> <li>• Crystallographic changes (A)</li> <li>• Change in energy levels (A, I)</li> <li>• Hole/electron transport layer degradation (I)</li> <li>• Dopant diffusion into active layer (I)</li> <li>• Change of uniformity of interlayers (I)</li> </ul>

each technology to the stress loads can vary largely. Degradation rates, mechanisms and failure modes depend on the materials chemistry, structuring of the cell stack and the packaging of each system. This section examines the technology-specific phenomena for solar cells and PV modules based on crystalline silicon (c-Si), CdTe and CIGS. For each technology, failure modes and degradation mechanisms are described in detail along with typical mitigation strategies.

## 2.1 | c-Si

Silicon, the second most abundant element on the earth's surface, is the most developed semiconductor material for PV applications and dominates the market.<sup>6</sup> Being one of the oldest PV technologies, its degradation mechanisms have been studied extensively.<sup>7–10</sup> In addition to common environmental and voltage stresses, the c-Si systems can also suffer from mechanical loads because silicon wafers are

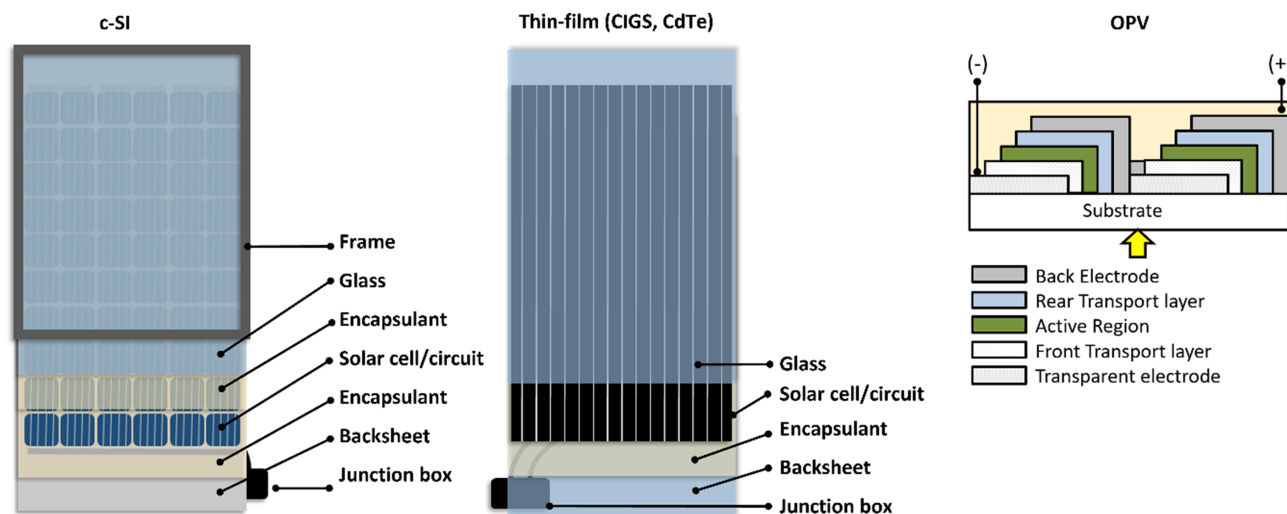


**FIGURE 1** Schematic diagrams of technologies discussed in Table 1. Note: Schematic diagrams of DSCs and MHPs are given in Sections 3.2 and 3.4, respectively. The OPV diagram shows a side perspective of a 2-cell monolithically connected module.

relatively stiff and brittle. This section examines the degradation mechanisms and features, such as cracks, snail trails, and hot spots, that could be induced by these stresses. We also discuss degradation modes that can be observed at c-Si PV systems, including potential induced degradation (PID), light induced degradation (LID) and light and elevated temperature induced degradation (LETID).

Until recently, most modules were based on polycrystalline or monocrystalline silicon cells with an aluminium back surface field (Al-BSF) structure. Now monocrystalline passivated emitter and rear contact (PERC) cells dominate the market, with several successor technologies already in development. Most notable among these are silicon heterojunction (SHJ), tunnel oxide passivated contact (TOPCon), interdigitated back contact (IBC) and tandem solar cells (typically c-Si coupled with a thin film PV technology). These technologies allow even higher efficiencies than PERC, though each has unique features that may lead to new degradation phenomena, such as damage to low temperature passivation layers in SHJ, shunts formed by conductive backsheets in IBC or sub-cell delamination in tandem cells. Sinha et al. studied the ultraviolet (UV) stability of different architectures of high-efficiency solar cells, although the cells were not encapsulated in order to increase the degradation rate during the test. The work shows that conventional Al-BSF cells were less susceptible to 340-nm UV degradation than SHJ, IBC and PERC-type cells. Their work showed that the rear side of bifacial cells exhibited greater photocurrent loss when compared to the front side, indicating a potential sensitivity of rear surface passivation to UV radiation.<sup>11,12</sup>

Moreover, after several years of unchanging wafer sizes (with  $156.75 \times 156.75 \text{ mm}^2$  wafers being standard), there is a rapid shift towards larger wafers, even up to  $210 \times 210 \text{ mm}^2$ . This continuous evolution of c-Si cell architecture, metallisation, interconnection, size, thickness and so forth means that module manufacturers must continually improve their understanding of module degradation and failure behaviour, as new modes can (and do) arise. In this section, the focus

will be on Al-BSF and PERC cells, of which the degradation and failure behaviour are best studied and understood through their significant field history. Generally speaking, further work is needed to understand the long-term stability of the newer silicon technologies.

### 2.1.1 | Cracked cells

The reduction of silicon wafer thickness aims to decrease the cost of silicon-based PV cells and modules. Nevertheless, the smaller thicknesses decrease the robustness of solar cells against mechanical loads and may cause cell cracking.<sup>13</sup> Cells that crack during the production process can be detected and eliminated. However, it is not possible to entirely avoid the formation of microcracks on the PV cells; therefore, it is crucial to quantify their long-term effects on the performance of PV modules, which is beginning to get more research interest. Microcracks and imperfections increase the risk of breakage during the production cycle and can propagate further during the lifetime of PV modules although they initially show little or no power loss.<sup>14,15</sup> There is some debate in the community on cell cracks as not all cracks result in a loss in performance; however, these can become larger with time and eventually lead to disconnections in parts of the cells.<sup>16–18</sup>

Microcracks may form in several stages, namely, during (1) ingot cutting, (2) production of cell and module, (3) transportation and installation and (4) operation of PV module due to environmental factors such as temperature cycles, wind, snow and hail.<sup>15,19,20</sup> Cracks interrupt the electrical conductivity in cell regions, which leads to reduction in the short-circuit current and the increase of the series resistance, resulting in output power reduction of PV modules<sup>21,22</sup> and can also increase PID.<sup>23</sup> The position, length and orientation of microcracks influence this power reduction.<sup>22</sup>

Cracks and microcracks are distinguished based on their size: A crack with a width up to  $30 \mu\text{m}$  is classified as a microcrack.<sup>24</sup> Cracks

occur in different shapes and sizes.<sup>25</sup> Cracks in c-Si PV cells and modules are further classified using other criteria such as severity and position<sup>21,26</sup> (see Table 2). Star-shaped cracks consist of several line cracks originating from an induced point. Line-shaped cracks are also initiated due to laser-cutting of wafers.<sup>27</sup> Figure 2 shows the classification of cracks according to their orientations in silicon PV cells.

When cells crack in the field, other degradation processes are likely to occur as well. K. Schulze et al. have attempted to quantify the impact of cell cracks. Their work estimates up to 20% power losses based on degradation analysis of more than 250 PV modules after 15-year operation, which were affected by cracks in combination with delamination and ethylene vinyl acetate (EVA) encapsulation browning.<sup>28</sup> In other studies,<sup>29,30</sup> experimental results have proven that cracking alone reduced the fill factor (FF) and output power up to 4% and 3% respectively.

### 2.1.2 | Snail trails

Crystalline-Si PV modules in the field may develop local line-shape discolorations, so-called snail trails, over the cells after a period of months to a few years; see Figure 3. Closer inspection shows that the discoloration occurs on the silver paste only. Snail trails form in the presence of cell cracks and depend on the packaging polymers (e.g., ethylene-vinyl acetate [EVA] acetic acid formation).<sup>31,32</sup> Moisture ingress seems to be the cause of silver line corrosion. Chemical reactions at the silver paste-encapsulant interface may lead to the formation of silver-containing nanoparticles above the silver lines.<sup>33</sup> The line conductivity is only reduced to a limited extent. Optical transmission loss is also negligible as the discoloration happens above the

silver lines; the encapsulant away from the silver line remains unaffected.<sup>33</sup> To observe snail trails in an accelerated test, a combination of mechanical load, UV exposure and temperature elevation is recommended.<sup>34,35</sup>

While the snail trail itself does not have a direct or significant effect on cell or module performance, it is an indication of moisture ingress, commonly caused by mechanical stress induced loss of module hermeticity and cell cracking. These are performance risks. Consequently, some reports indicate that the impact of snail trails on PV performance is negligible,<sup>36</sup> but other studies conclude that output energy produced by PV modules can be reduced up to 20% due to snail trails.<sup>37,38</sup> It appears that in the latter case, positive correlations between the occurrence of snail trails and power loss were misinterpreted as causal, whereas instead they have a common origin (moisture ingress, leading to more problems than snail trails alone).

### 2.1.3 | Hot spots

A hot spot is a high temperature area on the PV module that may cause serious damage on the solar cells and other elements on the modules (see Figure 4). In case of a mild hot spot, power loss might have a negligible effect on module performance, but if severe enough, it can burn the module packaging, causing complete failure. Furthermore, in minor hot spot issues, no power loss can be observed. In the case of silicon modules, heating is known to reduce the power output, so hot spots cause localised decreases in power output.<sup>40–42</sup> Hot spots are also likely to create localised temperature differences that, as a result of thermal expansion, could result in cell cracking or delamination.

**TABLE 2** Crack classification based on direction, position, size, shape and severity<sup>20</sup>

Direction	Position	Size	Shape	Severity
Diagonal	Facial	Macrocracks	Line shaped	Mode A:
Parallel to busbars	Subfacial	Microcracks	Star shaped	No significant power losses
Perpendicular to busbars				Mode B:
Multiple directions				Partially isolated and electrically inactive, causing power degradation and hot spot
				Mode C:
				Completely isolated and electrically inactive, causing power degradation and hot spot

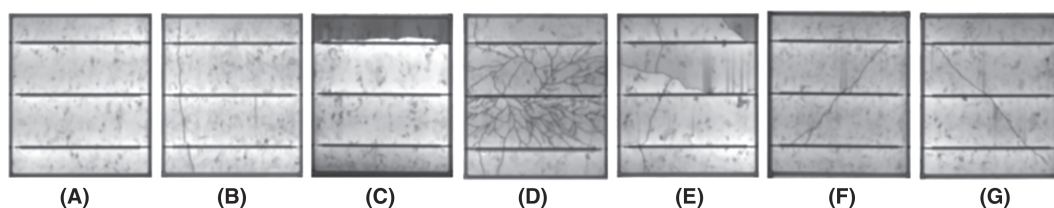


**FIGURE 2** Classification of cracks according to their orientations in silicon PV cells: (A) no crack, (B) perpendicular, (C) parallel, (D) dendritic, (E) multiple directions, (F) +45°, (G) −45° (reprinted from Papargyri et al.<sup>20</sup>)

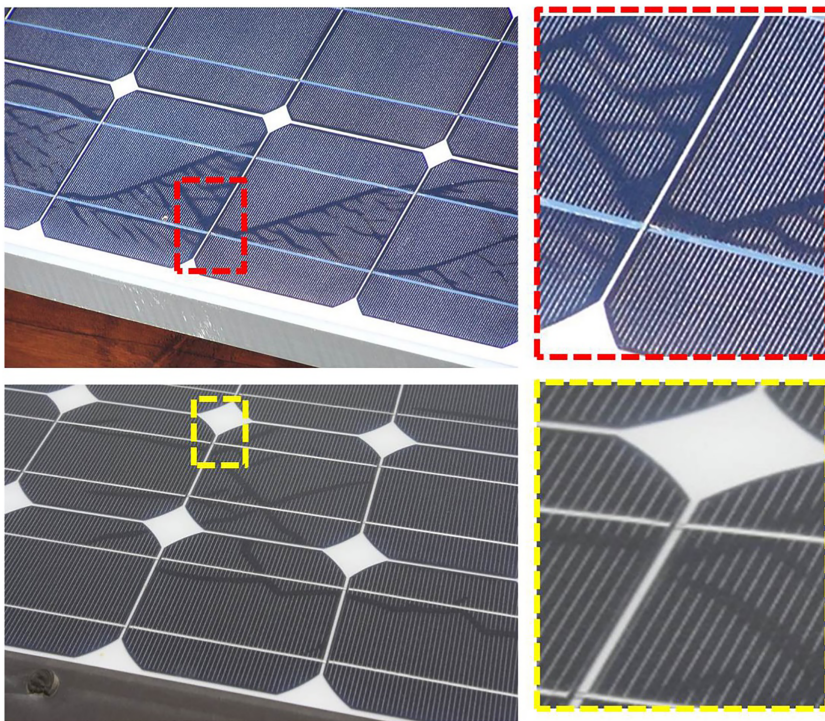


**FIGURE 3** The photograph of snail trails on PV modules<sup>39</sup>

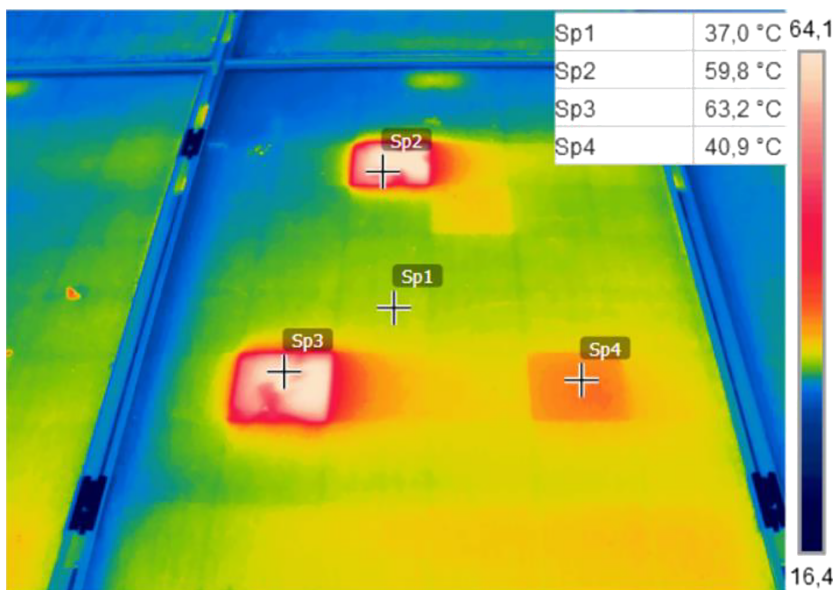


**FIGURE 4** Thermal infrared (IR) photograph of a PV module affected by hot spots<sup>53,54</sup>

A hot spot forms when one or more solar cells generate less current than the string current of a PV module. A hot spot can occur in a PV module due to various causes, such as cells mismatching, partial shading or interconnection failures.<sup>9,43–47</sup> Indeed, when the cell is affected by partial shading, it results in a short circuit condition or a reverse bias.<sup>45,48</sup>

An entire cell can form a hot spot in a module; alternatively, the cell temperature can also be non-uniform. Hot spots can occur within a cell in case of manufacturing defects, such as deformations at the p–n junction, a local impurity imbalance or metallurgical shunts.<sup>41,46,49–51</sup> Cells with such hot spots are normally identified and

rejected during cell testing, but they can also form over time due to cell and module degradation. They can appear when cracks form in silicon cells; hence, nonuniform distribution of the current in the fingers and busbars transpires. The localised heating may accelerate other degradation processes.<sup>20,52</sup>

#### 2.1.4 | PID

High potential differences over insulators, in the kilovolt range, tend to cause such insulators to fail. Small leakage currents and local

discharging may occur under these circumstances. PV modules are daisy-chained to improve power efficiency and lower the system cost. In that case, the potential difference between cells and frame may reach  $\sim 1000$  V, depending on the module, combiner and inverter ratings. This may soon even go as high as 1500 V, as some manufacturers are pushing to reduce the balance of system (BoS) cost.

Degradation phenomena in PV modules related to this high voltage are termed PID and typically lead to losses up to 5% but sometimes significantly more. PID degradation is primarily caused by the potential bias but is also affected by humidity and temperature. This is related to the leakage current between the frame and the cell. Recent work, which subjected c-Si PVs to PID testing under IEC 62804-1 standards, estimated that annual degradation was 11.2% per annum in a high humidity environment such as Miami (as opposed to 6.9% in a lower humidity environment).<sup>55</sup>

Discolouration, delamination, microcracks, shunts and even stacking faults are observed in c-Si leading to significant power and efficiency losses. The EL images after the PID stressing show that the degradation is strongest at the frame edges. The standard PID test procedure follows stressing the module with an external bias of 1000 V in a climate chamber of 60°C (or 85°C) and 85% relative humidity (RH) (IEC 62804-1).

The effect depends strongly on the magnitude and polarity of applied voltage. Two main mechanisms have been identified in PID of c-Si: (1) shunting (PID-s) and (2) surface polarisation (PID-p). In PID-s local shunts are formed over the emitter. This is typically worse under negative bias and for p-type wafers, because sodium ions from the cover glass migrate to the cell due to the external bias and get reduced to metallic sodium in the  $n^+$  emitter. Here, they decorate pre-existing stacking faults to form a conductive path between the n-doped emitter and p-doped base.<sup>56</sup>

On the other hand, PID-p results from a surface polarisation effect due to the accumulation of net charge in the dielectric stack between frame and cell, a typical case of high voltage creepage. This tends to be more common under positive bias and for n-type wafers. This accumulated charge modifies the surface field of the cell, leading to a reduction of short circuit current and open circuit voltage.<sup>57</sup> PID-p is a reversible phenomenon, if it is detected at an early stage in PV modules. However, the underlying physical mechanism of PID-p should be still investigated. In both cases, a strong recovery of the cells after the application of the high voltage stress test is observed. Presently not enough data are available to quantify the impact of this degradation mode in the field. More studies are needed to investigate this further.<sup>58-60</sup>

### 2.1.5 | LID, LETID and UV induced degradation (UVID)

LID and LETID are two phenomena that can be observed in c-Si systems and result in significant reduction of minority carrier lifetime in the bulk of c-Si wafers and the solar cells.<sup>61,62</sup> UVID is a related phenomenon, caused specifically by exposure to UV light. Each

mechanism can lead up to a few percent power loss, and some manufacturers have already developed mitigation or stabilisation strategies.

LID can occur even at low light exposure at room temperature, and the formation of a boron-oxygen and iron-boron defects in the silicon wafer are the main degradation mechanisms.<sup>61</sup> To mitigate the effects of LID, it has been proposed to decrease the oxygen content or substitute boron by other dopants such as gallium.<sup>62</sup>

LETID is a specific degradation type first observed on PERC-type multi-crystalline Si PVs in the field.<sup>63</sup> Later works showed that mono-Si cells also suffer from degradation under the combination of light and temperature stress. In comparison to LID, which occurs in a short period time of initial exposure to sunlight, LETID develops more slowly. The consequence is power loss up to several percent, though there can be a recovery over several years in warmer climates.<sup>64</sup> As in the case of LID, boron-oxygen complexes can be observed after LETID but are not the main root cause for degradation.<sup>63</sup> Hydrogen redistribution phenomena are currently considered responsible.<sup>64</sup> Preventive measures that can be taken for the mitigation of LETID include use of silicon wafers with low oxygen content, dielectrics with little hydrogen and low firing temperatures.

UVID was even more recently identified in c-Si. It is particularly apparent in modules with a UV pass encapsulant. It appears to affect mostly cells with passivated layers, such as variations of PERC, SHJ or TOPCon cells. UV can damage the cell passivation, leading to hydrogen loss at the surface and hot carrier damage in the bulk. The effect can be minimised by improving the composition and processing of passivation layers or using UV blocking encapsulants, though the latter method comes at the cost of lower cell power.<sup>12,65</sup>

## 2.2 | CdTe

CdTe technology dominates the thin film PV market based on the relatively low cost for manufacturing, increases in module efficiency (18%), small temperature coefficient (0.25%/°C) and large scale of manufacture.<sup>49</sup> The latter has been largely due to one manufacturer, First Solar, that now produces in excess of 5 GW per year. The history of CdTe module deployment is much shorter than that for c-Si so less is known about the long-term performance.

Wendlandt et al.<sup>50</sup> reported the range of measured degradation rates for CdTe modules to be 0.2–4%/year per year with a median value of 0.5%/year. The range can partly be attributed to variations in the manufacturing method and module sealing but is largely due to the non-linear development of CdTe module degradation with time.

The IEA-PVPS Report (2014)<sup>34</sup> mentions the main CdTe-specific failure mechanisms as being:

- Front glass breakage that can cause short term failure;
- Back contact degradation that causes longer-term loss of performance.

These are detailed in the following subsections. In addition, we will treat PID in CdTe modules.

## 2.2.1 | Front glass breakage

A consideration for CdTe PV technology is the constraint imposed on the manufacturing process by the superstrate configuration where the front glass is used as the substrate for depositing the thin films in the PV device. This prohibits hardening or tempering of the front glass (the superstrate) because it has to endure a series of temperature cycles during the deposition of the thin film coatings and heat treatment. The lack of hardening or tempering makes CdTe modules more susceptible to failure due to front impact (see Figure 5).<sup>66,67</sup>

## 2.2.2 | Back contact degradation

The role of copper in CdTe modules has been an important factor for reducing back contact series resistance and doping the CdTe absorber layer.<sup>68</sup> However, too much copper applied to the back surface will result in diffusion to the front junction and cause an increase in carrier recombination and loss in  $V_{oc}$ . Controlling the amount of copper applied to the back surface of CdTe is therefore crucial to obtain high efficiency devices. Artegiani et al.<sup>69</sup> present evidence that just 0.1 nm of Cu suffices. The drop in PV module performance over the first 2–3 years of deployment is attributed to copper diffusion to the front junction. As Perrenoud et al.<sup>68</sup> have pointed out, the solubility of copper in CdTe is low; Cu concentrates at the crystal grain boundaries, which provide a fast diffusion pathway to the front junction.

The temperature coefficient of CdTe is  $-0.25\%$  per  $^{\circ}\text{C}$  temperature rise, half that of c-Si. That makes CdTe an attractive choice in warm climates; however, the high operating temperatures could enhance the diffusion of copper. Strevel et al.<sup>70</sup> have observed a 4–7% power loss over the first 1–2 years before a linear degradation factor of  $-0.7\%/year$  is established. The initial drop goes faster at higher operating temperatures. Strevel et al. state that the initial power output of the module is underspecified to deal with this initial degradation.

In a series of controlled laboratory heat cycling tests on experimental CdTe solar cells, Bertinello et al.<sup>71</sup> have attributed degradation to two different mechanisms. The first is copper diffusion, and

the second is oxidation. One of the observations was an increase in series resistance, which was attributed to loss of copper from the back contact accompanied by a conversion of low resistance  $\text{Cu}_2\text{Te}$  to high resistance CuTe. The diffusion of the excess copper through the CdTe to the CdS buffer layer causes loss of short wavelength external quantum efficiency. The oxygen ingress during accelerated heat testing caused the formation of TeO at the back contact, increasing resistance. However, in a paper on As doped CdTe, an air anneal resulted in enhancement of the  $V_{oc}$ .<sup>72</sup> The oxidation degradation might occur specifically to Cu doped back contacts.

A radical solution to copper-related degradation is to replace Cu by another element, preferably one with a higher solubility, to obtain higher acceptor concentrations. With As doping, this concentration has been shown to exceed  $1 \times 10^{16} \text{ cm}^{-3}$ .<sup>73,74</sup> Arsenic is a slow diffuser in CdTe solar cells and does not appear to diffuse into the buffer layer so it should improve the long-term stability. Experimental arsenic doped CdTe modules have now undergone the standard thermal stress test subjected to conventional Cu doped modules.<sup>73</sup> Remarkably, the As doped modules show an initial rise in efficiency over the same period that the Cu doped module shows the steep decrease mentioned earlier. This is followed by an efficiency constant over time, bearing the prospect of an improved long-term performance.

## 2.2.3 | PID

Like c-Si modules, PID in CdTe modules is also strongest on the negative string end.<sup>75</sup> Modules from a 2.3-MW CdTe plant that had been operational for 6 years showed 43% power loss compared to the nominal power on the negative end and 17% power loss on the positive string end; the latter probably unrelated to PID. PID degradation came with visible transparent conducting oxide (TCO)-corrosion around the clamps and edge region. In some cases, the reverse bias protection had failed.

As with c-Si solar modules, the mechanisms governing PID in CdTe modules are not yet fully understood. Leakage currents develop due to the large potential difference between the grounded frame and the cells, particularly those at negative potential. The glass

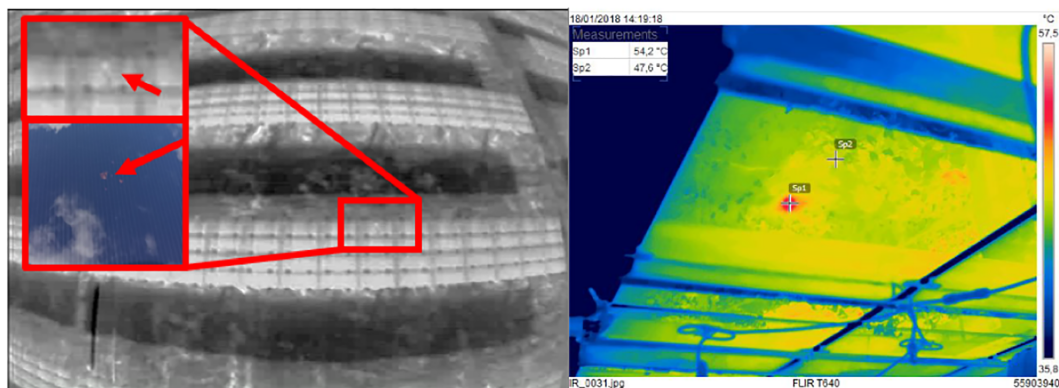


**FIGURE 5** A hot spot due to cracked front glass (not readily spotted by visual inspection) detected using aerial infrared thermography<sup>66,67</sup>

superstrate for CdTe modules is typically a soda-lime glass, and sodium can migrate towards the cell and reach the junction region degrading cell performance by introduction of recombination centres. This typically degrades the  $V_{oc}$  and FF of the cell. The mechanism of ‘Na transport’ and the subsequent cell degradation depend on the moisture conditions. In a dry climate, the sodium migration described above will operate and can be reversed by subjecting the modules to a reverse bias. Moisture ingress however will result in irreversible degradation of the module as the reduced sodium will react with the moisture to produce atomic hydrogen, which will then react with the  $\text{SnO}_2$ -based TCO. This is the mechanism that leads to visible TCO degradation near the edges of a module (see Figure 6).

### 2.3 | Copper indium gallium diselenide (CIGS)

CIGS is now one of the most mature thin-film PV technologies with rapid growth of installations and production capacity, which is due to

its low fabrication costs, short energy payback time and most importantly due to their freedom of size, shape and flexibility, making CIGS suitable for integration in various infrastructures.<sup>77</sup> Jordan et al. reported that CIGS modules installed in the 21st century demonstrated low median power degradation rates of 0.5% per year.<sup>78</sup> The majority of the modules showed rates between 0% and 1% per year, while some modules actually improved during outdoor operation. A small quantity of outlier modules showed worse field behaviour.

Degradation in CIGS PV systems can be induced by various stress loads including humidity, partial shading and biases. CIGS solar devices are formed as a multi-layered material stack and responses to such stress loads differ for each layer. Figure 7 demonstrates the cross-sectional schematic of the material stack in a typical CIGS monolithically interconnected device and illustrates the degradation mechanisms. P1, P2 and P3 denote the presence of so-called scribes (patterning lines), which are necessary for module formation.<sup>79,80</sup>

This following subsections discuss these particular failure mechanisms in detail under following subsections:

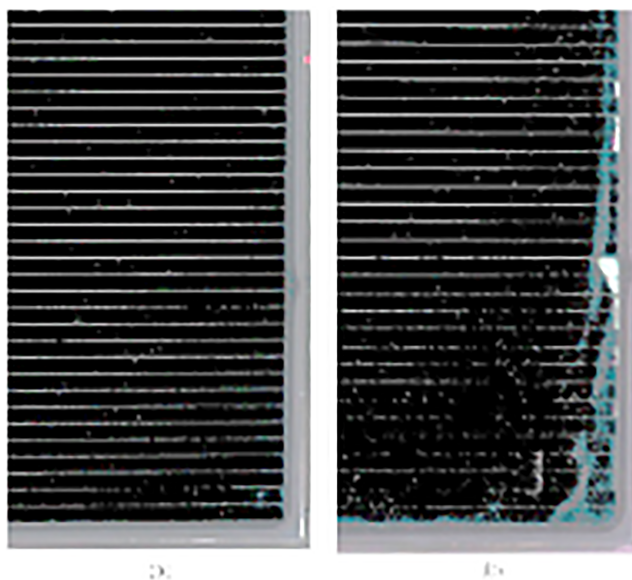


**FIGURE 6** Images of a CdTe module (A) before and (B) after 1043 h of voltage stress of  $-1000$  V in a chamber of  $85^\circ\text{C}/85\%RH$ , the latter exhibiting TCO corrosion<sup>76</sup>

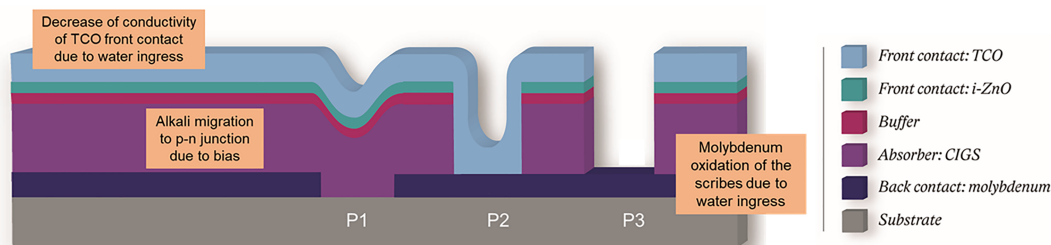


**FIGURE 7** Schematic representation of a typical CIGS solar device and the degradation mechanisms that can occur in an unpackaged CIGS solar cell due to damp heat exposure and internal or external biases. This figure is based on figures from other studies<sup>81–84</sup>

- Decrease of conductivity of TCO front contact and molybdenum oxidation of the scribes due to water ingress
- Alkali element migration promoted by internal (under illumination) and external biases (PID)
- Wormlike defect formation due to partial shading.

### 2.3.1 | Reduction of contact conductivity due to water ingress

In order to study the impact of humidity, many studies have looked at the performance loss of CIGS devices without any packaging under damp heat conditions (85°C/85% RH). In this way, the intrinsic stability of the solar cells and minimodules could be studied. A literature review<sup>80</sup> revealed strongly varying degradation rates under these damp heat conditions. The most impacted device parameters were the FF and the open circuit voltage. These devices were on the other hand mostly stable when exposed to dry heat conditions, which was also the case for packaged devices exposed to damp heat. This indicates that adequate packaging, both flexible and rigid, is sufficient to keep the devices stable. Nevertheless, in case of insufficient water protection, like a damaged edge seal or a broken front sheet, humidity could enter a CIGS device. This can have a negative impact on especially the conductivity of the front contact and the monolithic interconnection.

In CIGS devices, several types of transparent conductive oxides (TCOs) are used as front electrode. Sputtered aluminium doped zinc oxide (ZnO:Al) is the most common material, while sputtered tin doped indium tin oxide (ITO) can be implemented as well.

In the case of non-encapsulated CIGS solar cells, thus allowing water ingress, increased resistivity of ZnO:Al is often found to be a major cause for efficiency loss, and even a minor resistivity increase will directly impact the device performance due to series resistance increases.<sup>80</sup> Damp heat related resistivity increase of ZnO:Al is primarily caused by a decrease of carrier mobility due to grain boundary degradation. This is typically caused by the diffusion of 'foreign' species, like water and CO<sub>2</sub>, from the environment into the grain boundaries,<sup>81,82</sup> where the potential barrier can then increase.<sup>85,86</sup> The resistivity increase was reported to be largely reversible by annealing in vacuum<sup>87</sup> or in a reducing atmosphere at elevated temperatures.<sup>88</sup>

The more expensive ITO is generally more stable than ZnO:Al in the presence of humidity and elevated temperatures. Degradation of ITO can be caused by the migration of water and alkaline species into the layer leading to electrochemical instability. Temperature-humidity stress of this material was further shown to cause recrystallisation and local concentrations of In and Sn.<sup>89</sup>

Another effect that can occur in the presence of humidity is the degradation of the conductive molybdenum film, which functions as the back contact. This material can oxidise if directly exposed to (liquid) water and oxygen, especially under elevated temperatures. Oxidation can first lead to the formation of black and blue stains on the metallic molybdenum surface, which can contain

molybdenum oxide (MoO<sub>2</sub>/MoO<sub>3</sub>, potentially with sodium or selenium<sup>90</sup>). These materials can be badly conducting and/or poorly reflecting.<sup>83,84</sup>

This oxidation can mainly affect the scribes of monolithically interconnected devices, while it will not likely occur in the covered molybdenum back contact in the bulk of the material, due to the lack of direct water. In the location of the second scribe (see Figure 7, location P2), where a Mo/ZnO:Al contact is responsible for the current transport between solar cells, increased resistance of the scribe has been observed in model systems exposed to damp heat conditions.<sup>79,91-93</sup> Possible explanations are the introduction of an oxide layer at the Mo/ZnO:Al interface as well as increased resistivity of ZnO:Al in this scribe.<sup>80</sup> Moreover, oxidation of the P3 scribe was also observed, for example on positions that have been damaged by the scribing process. As long as some conductive molybdenum is present, this is not per se a problem: If the layer is only partly degraded, the current can still laterally bypass via a non-degraded part.<sup>93</sup> However, in extreme cases, the molybdenum in the P3 can completely disappear, leading to the loss of connection between the cells.

### 2.3.2 | Alkali element migration and PID

Alkali elements, in particular sodium, are highly available in CIGS solar devices as the cover glass and the substrate glass are both typically soda-lime glasses containing more than 15% Na<sub>2</sub>O. The efficiencies of CIGS devices are known to improve by sodium doping through defect passivation at grain boundaries; however, the presence of alkali elements can be detrimental depending on their quantity and distribution within the solar stack.

Theelen et al.<sup>94,95</sup> demonstrated that combined exposure to damp heat and illumination (leading to a small bias voltage over the cell) of unpackaged cells led to migration of the alkali elements sodium and to a lesser extent potassium. It was proposed that humidity leads to liberation of the alkali elements from the grain boundaries within the polycrystalline CIGS absorber, allowing movement of these species. They can then end in the p-n junction and ZnO:Al front contact and have a negative impact on the shunt resistance.

The migration of alkali elements can also be induced by an external voltage stress and can lead to PID as in the case of c-Si and CdTe PV systems. When compared under the same testing conditions, it was demonstrated that CIGS thin-film PV modules have higher resistance to PID than multicrystalline Si and a-Si modules.<sup>96</sup>

PID in CIGS PV systems depends on the migration behaviour of sodium. Sodium either migrates from the substrate glass and accumulates at CIGS/CdS interface deteriorating the p-n junction or migrates to ZnO:Al front contact layer from the cover glass causing its corrosion or delamination.<sup>96,97</sup> The accumulation of sodium can result in reduction in charge carrier concentration and built-in voltage, TCO corrosion and a degree of shunting, resulting in a significant drop in open circuit voltage  $V_{oc}$  and FF.<sup>98</sup> A lower intensity of EL is observed at the degraded regions, which are mostly at the edge cells closer to the frame (see Figure 8).<sup>76</sup>

**FIGURE 8** Optical images of CIGS solar modules (A) before and (B) after PID test of 1043 h in a chamber of 85°C and 85% RH and –1000 V. TCO corrosion is shown by the blue arrows and (C) is an electroluminescence (EL) image of the state of (B).<sup>76</sup>

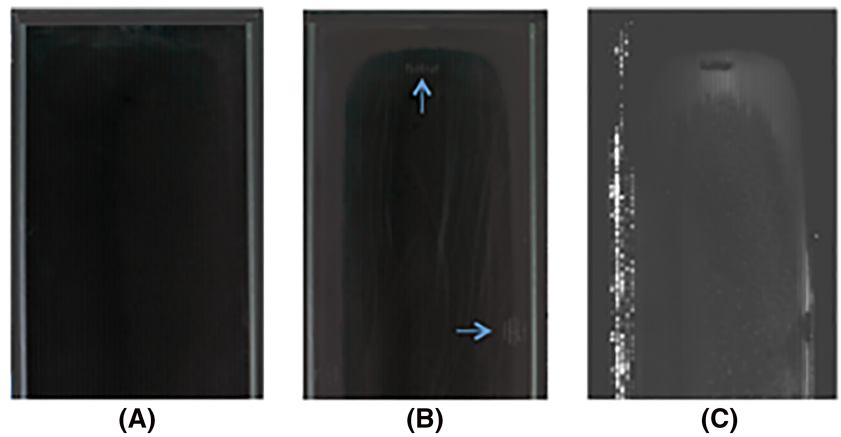


**FIGURE 9** A close-up image of worm like defects in two interconnected cells of a CIGS module exposed to partial shading stress. Reprinted with permission of Bakker et al.<sup>104</sup>

### 2.3.3 | Partial shading

The impact of partial shading strongly depends on the design of the module. Commercial CIGS modules can be divided into two classes. The first class consists of separated large cells with a current collecting grid in either series or parallel connection. Such modules may commonly experience (changing) partial shading, as they are very attractive for integration in for examples vehicles, textile and facades. However, this module design allows the use of bypass diodes, so the negative impact of partial shading can be minimised. Rigid monolithically interconnected modules form the second class. They consist of series connected long, narrow cells (e.g. 1200 × 5 mm). In general, these modules maintain a very good output power when partly shaded,<sup>99</sup> especially when it comes to predictable row-to-row shading.<sup>94</sup> However, negative long-term effects can occur when the

orientation of the cells is such that one or more cells are completely shaded, while other cells are illuminated. These modules generally do not contain bypass diodes.

For the monolithically interconnected modules, very harsh partial shading can thus present a risk, due to reverse bias exposure. An example of an undesirable situation is the use of a cleaning robot, which can completely cover one or more cells while the modules are still operational. Such shadings can result in the non-reversible formation of wormlike defects, which are formed by a hot spot that propagates over the cell area. These long and winding defects have a width of tens of micrometres and can have a length of multiple centimetres (see Figure 9). In these defects, the CIGS absorber material has recrystallised and formed into a thick semi-porous and likely conductive structure. Due to the volume expansion, a ‘ridge’ of elevated material<sup>100–102</sup> is formed. At these positions, the front

contact is still intact but is lifted from its original position. The appearance of wormlike defects leads to the formation of localised shunts in the devices, negatively affecting the module output. Although the performance loss of one wormlike defect can be minor, repeated exposure to harsh partial shades will lead to multiplication of the losses.<sup>103,104</sup> Alongside to wormlike defects, also non-permanent changes in device performance were observed due to (mild) reverse bias exposure.<sup>105</sup> Since these effects were often reversible, for example for small cells under illumination,<sup>106</sup> they are not often studied.

Various studies have reported on design solutions for the mitigation of the impact of (large) reverse biases, especially to prevent the formation of these wormlike defects in monolithically interconnected modules.<sup>107,108</sup> On the other hand, changes in the composition or thickness of the layers in the cell stack can also impact the cell behaviour under reverse bias.<sup>100,109–111</sup> More information about the impact and the mitigation of partial shading can be found in the review article by Bakker et al.<sup>104</sup>

## 3 | EMERGING TECHNOLOGIES

### 3.1 | Introduction

Having discussed the well characterised problems and mitigating strategies employed in mature technologies, this section will describe what is currently known for emerging technologies and therefore guide the reader to what are the potential stumbling blocks of emerging technologies. There is a much greater focus at the moment on intrinsic device-related factors rather than on process related failures or long-term issues such as device encapsulation. This is not surprising as the inherent material instabilities need to be better understood and the reliability improved before the challenges of longer-term instability associated with module level accelerated and outdoor testing are undertaken.

Emerging PV technologies aim to drastically reduce the materials cost and the energy payback time as compared to the technologies in mass production. Many papers indicate that the greenhouse gas emissions from the emerging technologies would improve tremendously (and proportionally) when longer lifetimes are achieved than presently possible.<sup>112</sup> Inorganic materials are being replaced by organic materials where possible and roll-to-roll fabrication techniques are being adopted to fabricate large area PV modules at low cost. Arguably, the use of organic materials offers opportunities for tuning of functional properties, but it also introduces numerous degradation and scale-up issues. Among the wide range of emerging PV technologies, three main classes can be distinguished: DSCs, OPVs and perovskite-based solar cells (MHPs). Among the emerging technologies, MHPs outperform in terms of performance and scientific activity, in spite of being a new entry in this category. Thus, in this review, we will mainly focus on MHPs; however, it is important to note that the MHPs field leans heavily on the knowledge and experience built up from the DSC and OPV.

### 3.2 | DSCs

The DSC was first reported by O'Regan and Grätzel in 1991<sup>113</sup> and may still have a role to play in energy generation for emerging indoor applications.<sup>114</sup> The indoor efficiency of DSCs is very impressive (e.g. 28.9% at 1000 lux).<sup>115</sup> However, the AM1.5G certified performance is still only 12.25% (0.0963 cm<sup>2</sup> aperture area) and decreases down to 8.8% for a sub-module (398.8 cm<sup>2</sup> device area),<sup>116</sup> as a result of absorption limitations.

#### 3.2.1 | Device architecture

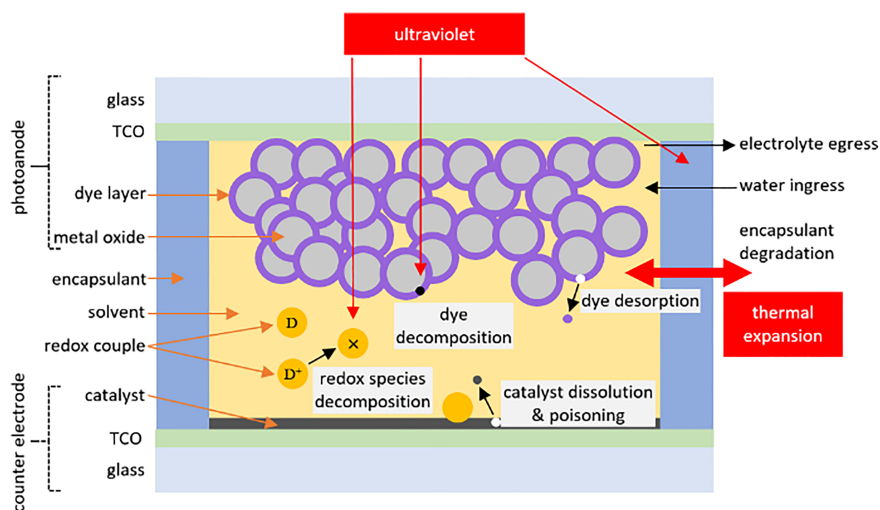
The DSC has several components; the photon absorption occurs within a dye molecule and charge separation and collection are a result from interfacing materials.<sup>117</sup> The remaining components that make up a DSC are the anode and cathode substrates, the anode and cathode electrodes, the electrolyte, and the encapsulant (see Figure 10). The anode and cathode substrates can be transparent (e.g., glass, PET and PEN) or opaque (metallic). However, DSCs can be made on substrates that can be engineered to be thin and thus lightweight and flexible.<sup>118</sup> In a conventional DSC, the anode is where light absorption and charge separation occur and thus is referred to as the photoanode. Transparent substrates are typically glass, PET or PEN. For non-metallic substrates, a deposited TCO layer is necessary. An n-type porous metal-oxide is deposited onto the conducting substrate. The metal-oxide is subsequently sensitised by adsorbing the dye onto its surface. Similarly to the anode, the cathode can use a metallic or TCO coated transparent substrate. Here, a catalyst layer is required for efficient electrolyte regeneration. The electrolyte is a redox couple dissolved in an organic or aqueous solvent. A thermoplastic hot-melt or a glass frit<sup>119</sup> holds the cathode and anode together. This also acts as the electrode spacer to prevent electrode short-circuiting.

There are a significant number of up-to-date reviews that describe in depth the DSC (Vlachopoulos and Hagfeldt<sup>117</sup> is a recent example—a list of reviews can also be found within). The stress factors for the DSC are essentially the same as other technologies although the added complexity is the impact of electrolyte solvent egress and electrolyte corrosiveness (see Figure 10). We next describe the degradation pathways each of the device components suffers from when exposed to stress factors.

#### 3.2.2 | Photoanode

Dye stability is the limiting factor for the photoanode.<sup>120</sup> Water presence can lead to dye desorption by hydrolysis. Water can be present during device sealing or ingress over time. Using hydrophobic dyes has shown promise in reducing this challenge.<sup>120</sup> Also, a promising alternative are hydrophilic dyes that function in aqueous electrolyte media,<sup>121</sup> thus eliminating the need to prevent water ingress. If UV light is permitted to enter the photoanode, photocatalytic degradation of the dye also occurs mediated by the high band-gap metal-oxide.<sup>122</sup>

**FIGURE 10** Bi-facial dye solar cell schematic showing main operating components, stress factors and resultant degradation mechanisms. In this example, the photoanode is composed of the TCO coated glass and dye sensitised metal-oxide. The electrolyte is composed of a redox couple  $D/D^+$  ( $e^-$  donor/oxidised  $e^-$  donor species). The counter electrode is TCO coated glass coated with a catalyst.



### 3.2.3 | Counter electrode

For a conventional DSC, the cathode contains platinum that over time degrades either by dissolution or by redox species poisoning (e.g.  $I^-/I_3^-$  electrolytes).<sup>123</sup> Of all DSC components, the counter electrode (in a conventional photoanode configuration) is where the least research has gone into evaluating stability. Pt-based counter electrodes are not economically viable. As such, there are several reported alternatives,<sup>123</sup> ranging from other metals and alloys, conducting polymers, carbon materials, transition metal compounds and hybrids. Polymer-based counter electrodes can be considered the most promising alternative because they can be low-cost, transparent and flexible, while still exhibiting equivalent or superior catalytic activity. One can argue that the counter-electrode is the final piece of the jigsaw puzzle which is a DSC, and thus, its development direction will depend on the dye/electrolyte combination.

### 3.2.4 | Electrolyte

The electrolyte is composed of a solvent (organic or aqueous) and a redox shuttle. Volatile organic solvents are inherently difficult to encapsulate. Solvent egress not only degrades device performance, but there are safety (e.g. flammability) and environmental concerns. High boiling point solvents, room temperature ionic liquids, gel electrolytes or even electrolyte substitution for solid state hole-transporting materials are alternatives.<sup>124</sup> However, these come at the detriment of cost, lower efficiencies or lack of transparency (necessary for bi-facial configurations). Aqueous-based electrolytes appear to be inevitable for DSC commercialisation because of the potential for easing the encapsulation requirements while also rendering this class of device as safe. Though efficiencies are still below 10%, progress may be rapid.<sup>125,126</sup>

Traditionally, the iodide/triiodide  $I^-/I_3^-$  redox couple has been the choice for high performing DSCs. However, its corrosive nature towards Ag, Cu, Al and stainless steel imposes restrictions.<sup>123</sup>

Introducing cobalt redox mediators Co(ii)/(iii) resulted in a significant increase in efficiencies (from certified approximately 11% to the current AM1.5G record of over 14%,<sup>127</sup> though uncertified). However, stability is poor and is attributed to photosensitivity.<sup>128</sup> Promising alternatives are copper Cu(ii)/(i) redox mediators,<sup>123</sup> demonstrating superior indoor efficiencies,<sup>115</sup> and showing promising high temperature and light soaking stability.<sup>129</sup>

### 3.2.5 | Encapsulation

Device encapsulation is achieved by the anode and cathode substrates and the adhesive material that is used to sandwich these together. The substrates prevent water ingress and also contain the electrolyte. Glass is by far the best material for both purposes. PET and PEN are permeable to water and oxygen ingress and also to the egress of volatile organic electrolyte solvents. How this affects device stability has been covered above. The plastic substrates are also unstable under UV. Metallic substrates require electrolyte corrosion resistance, raising costs.<sup>123</sup>

The bonding material must maintain stable physical properties in the device's working temperature range and withstand the pressure caused by the electrolyte volumetric thermal expansion. The thermal hot-melt is sensitive to UV exposure. The glass frit method although encouraging requires high annealing temperatures (600°C), which has the drawback of not being compatible with most flexible substrates.<sup>119</sup> Further lamination can be used to fully encapsulate the device to protect it from external contamination and UV exposure.<sup>130</sup>

### 3.2.6 | State of the art stability measurements

A recent review by Tiihonen et al.<sup>131</sup> was very critical of stability reporting for DSCs. They conclude that the major shortcomings are the inadequate group size for statistical analysis and deficient reporting of measurement conditions. Also, frequently missing are UV

intensities and humidity levels. They also point out that when attempts are made to demonstrate stability, success has only been achieved either at moderate temperatures (50–60°C) under light soaking or at high temperatures (80°C) but without light soaking. High temperatures combined with light soaking have always led to fast performance degradation. Outdoor ageing testing reports are also limited.<sup>131</sup>

Until recently, DSC research lacked well defined protocols for determining device power conversion efficiencies,<sup>132</sup> to the detriment of reproducibility. Consensus for stability testing of DSC is still lacking unlike for the perovskite and organic solar cells.<sup>131</sup>

In summary, no DSC device configuration has proved stability and reliability in accelerated testing to simulate outdoor conditions when all stress factors are present. However, the race is still on to develop sustainable efficient DSCs, which may in part synergistically solve some of the stability problems. Also, a portion of the DSC research community has become very critical of shortcomings in stability studies. This can be viewed as a positive sign.

### 3.3 | OPVs

OPV offers the possibility of producing flexible, large-area, semi-transparent, coloured PV modules using low-cost solution processing methods and is attractive for many applications including Building Integrated PVs and indoor modules. From an environmental perspective, they also possess the lowest embodied energy of any PV technology.<sup>133,134</sup> Most modern devices are based on bulk heterojunction cells and the at standard AM1.5 test conditions<sup>135</sup> and efficiencies of up to 31% under indoor lighting conditions.<sup>136</sup> Extending the lifetime of OPVs is vital in order to realise their feasibility for commercial applications.

In 2011, consensus standards were developed by the OPV community to provide a common framework to comprehensibly assess stability, as the IEC standards were considered too harsh to be considered meaningful.<sup>137</sup> A series of interlaboratory studies have been conducted on the stability of OPV devices. These papers highlight the complex relationships between materials, technological steps, degradation protocols and PV properties.

As with other technologies, the degradation of OPV solar cells is related to several stress factors that can be separated into both extrinsic and intrinsic factors. The intrinsic factors included the metastable morphology, stability of materials, the diffusion of the electrodes and buffer layers into the active material (see Table 1 for a fuller list); whereas the extrinsic factors include many of the same factors as other technologies (oxygen and water infiltration, irradiation, heating).<sup>138–140</sup> However, most OPV modules are made onto flexible substrates so bending is an additional mechanical stress factor.<sup>141</sup> There have been several review articles on OPV stability, and it is clear that degradation is also not due to a single intrinsic or extrinsic failure mechanism.<sup>142</sup> For example, this has been demonstrated by consideration of the combined effect of humidity and temperature on OPV degradation, leading to an interaction effect. When an OPV is

stressed by both temperature and humidity, a greater degradation is observed than when each factor is increased individually.<sup>143</sup> Furthermore, by not considering the interaction effects in other reports, misleading conclusions can be reached due to the significant impact interactions have on the rate of degradation.<sup>144</sup> The effects of applying multiple stress factors on OPV modules simultaneously using a design of experiment approach were performed to demonstrate predictive ageing of OPVs based on multi-stress testing using a log-linear life model.<sup>145</sup>

There has been a large body of research aimed at improving the stability; this has focused on active material design, device engineering of the active layers, employing an inverted architecture, transport layer optimisation, electrodes and encapsulation optimisation. However, from such a review, ranking of the different intrinsic and extrinsic factors is difficult in terms of severity; machine learning, however, presents a possible methodology for considering such literature sources and using analytical techniques to quantify and rank the significance of each factor.<sup>146–148</sup> Nevertheless, there are a number of examples where high stabilities have been reported. Non-fullerene acceptors (NFAs), namely, IDTBR and IDFBR, have been combined with the donor polymer, PBDDTT-EFT (PCE10), and devices were found to be highly efficient owing to changes in the microstructure, which reduces charge recombination and increases photovoltage.<sup>149</sup> Recent results published in<sup>150</sup> show that the lifetime of OPVs based on NFAs can remain within 80% of the initial power conversion efficiency (PCE) after 11 000 h under 1 Sun illumination. In this work, it was stated that the photo-stability is strongly dependent on the end-groups and side-chains of the NFAs, and the side-chain modification can significantly improve the morphological stability. Nevertheless, the results were obtained in samples with only 10.4 mm<sup>2</sup> active area. Despite these highly encouraging recent results, the next challenge is to scale this efficiency and stability to larger area modules.

One noticeable trait in the OPV community (as with the DSC and MHP ones) is that outdoor monitoring has been a sparingly adopted approach for testing the stability. By testing emerging PVs in outdoor conditions, multiple stress factors can be applied, and outdoor testing remains one of the best approaches to review stability as the PVs are subjected to multiple stress factors<sup>151,152</sup> including tests that aren't conducted in ISOS consensus standards such as the impact of condensation.<sup>153</sup> One of earliest reports on outdoor testing of OPVs was conducted by Katz et al. in 2007.<sup>154</sup> A number of outdoor stability studies were led by the Danish Technical University (DTU) on polymer-based OPVs, and Josey et al. have conducted studies on evaporative, small molecule OPVs.<sup>155,156</sup> One of the most significant was the report on a solar park based on polymer solar cells, which investigated the practicality of assembly, the installation, operation and end of life. In this work, analysis showed that very high voltage installations are formed, due to the large number of serially connected cells, and the effect of this high voltage on performance should warrant further stability studies.

In addition, new research directions are discussed by Krebs et al. whereby advanced materials must be developed with the potential for large scale application in solar parks, fast roll-to-roll processing using

only abundant materials and finally the use of flexible substrates with low-cost barriers and adhesives. Finally, Krebs et al. noted how this research field could be directed by life cycle assessment (LCA) and that a short energy payback time of the order of 1 day could be obtained by choosing a wooden support structure, roll-based installation and high voltage connections, assuming mass manufacturing.<sup>157</sup> This suggests that emerging technologies may actually require much less than 30–50 years of stability if there is a paradigm shift in manufacturing, installation and recycling.

### 3.4 | Metal halide perovskite (MHP) solar cells

#### 3.4.1 | State of the art progress

MHPs have emerged as a new class of semiconductors to fabricate low-cost and efficient PV devices. The term 'organic-inorganic metal halide perovskites' is used to describe a group of compounds, which has a structure similar to  $\text{CaTiO}_3$  and is represented by  $\text{ABX}_3$ . Here, A is typically an organic alkyl ammonium cation or Cs, B is a metal e.g., Pb, Sn and X is a halide anion.<sup>158</sup> MHPs are relatively new to the PV community and entered in 2009 as a promising material.<sup>159</sup> From the initial reports with a PCE of 3.8%<sup>159</sup> in a dye solar cell architecture, the PCE has witnessed rapid increase. The current certified record PCE is 25.5% for single junction and >29% for tandem (perovskite over Silicon) solar cells.<sup>160–162</sup>

These high efficiencies are possible because perovskites possess extraordinary intrinsic optoelectronic properties such as broad absorption spectrum, high absorption coefficient enabling low binding energy, long charge-carrier diffusion length and long carrier separation lifetime, which makes them promising materials for PV. Moreover, they offer flexibility, semi-transparency, low mass and are easy to synthesise. The precursor materials for the synthesis of perovskites such as methyl ammonium (MA), formamidinium (FA) and lead halides are low cost, and their processing is relatively simple.

Despite the success in research, most of the achievements result from laboratory studies, and the higher performance still needs to be validated for commercial PV. Particularly by addressing the reliability challenge, it has the merits to surpass the silicon baseline. There is also an appealing industrial rationale for tandem cells, either together with silicon or CIGS or in the form of a perovskite-perovskite tandem. The operational stability of the first MHPs<sup>159</sup> was in the order of minutes rather than hours, and this has improved from minutes to days, to weeks, when the liquid electrolyte was replaced with a solid-state hole conductor, compositional engineering of perovskites,<sup>163,164</sup> passivation of perovskites and rational charge selective layers. In view of these rapid developments, it is not difficult to envisage that MHP will achieve a 25-year life time warranty, which is common for commercial silicon PV modules.

Typically, the efficient lead-based MHPs display a bandgap close to 1.5 eV, and lowering the bandgap further will be of importance. By substituting the Pb with Sn, a reduced bandgap can be obtained, and mixed Pb-Sn-based perovskites are potentially attractive to achieve

the bandgap value of 1.2–1.3 eV. The energy gap is in the ideal range and is suited for perovskite-perovskite tandem application.<sup>165</sup> It is a known fact that the use of Sn-based MHPs compromises device reliability, owing to the oxidation of  $\text{Sn}^{2+}$  to  $\text{Sn}^{4+}$ . The relative ease of oxidation of  $\text{Sn}^{2+}$  to  $\text{Sn}^{4+}$  led to an increase in the Sn vacancy density, which, in turn, lowered the carrier lifetime and diffusion length. Such oxidation can easily be triggered from the atmospheric oxygen or the solvent used. To suppress this oxidation, the use of reducing agents, such as metallic Sn powder, hypophosphorous acid, the vapour of hydrazine and phenylhydrazine hydrochloride, and other antioxidants and mild acid was reported. By suppressing the oxidation processes, a PCE for Sn-Pb MHPs of 21.7% has been reported.<sup>166</sup> Similarly, to suppress the  $\text{Sn}^{2+}$  oxidation, a bifunctional additive, that is, zwitterionic antioxidant and formamidine sulfinic acid, and defect passivation of grain at the surfaces were reported by Xiao et al. All-perovskite tandem solar cells with 24.2% certified efficiency and area over 1  $\text{cm}^2$  use this surface-anchoring zwitterionic antioxidant.<sup>167</sup> Currently, the performance of Sn-Pb-based mixed MHPs is lower than that of lead halide-based MHPs, mainly due to poor carrier dynamics at the interfaces with the charge collection layers, and this can be overcome by the use of charge selective layers by minimising the energy level mismatch.

Common triggers for failure include heat, moisture, UV light (*discussed in the next section*) and compositional dynamics, such as ion migration, defect accumulation and phase instabilities of perovskites with mixed compositions. Such factors cause irreversible degradation and should be taken in to account during the measurements. Currently, competitive operational stability of over 1000 h during maximum power point tracking (MPPT) has been reported.

The MHPs Database Project<sup>168</sup> contains most of the MHP data available in the literature (from around 16 000 papers) and aims to collect all future device data in one place. So far, it is the most comprehensive data source available. In Figure 11A, the performance of devices at the end of the stability measurement is plotted as a function of total exposure time for all the samples in the database, regardless of perovskite composition, cell architecture, stack sequence, perovskite composition, initial efficiency and testing condition. It can be deduced from Figure 11A that a lot of cells degrade relatively rapidly and that measurement times only seldom go beyond 1500 h but that there are examples of cells (<5% of the database) that are stable for thousands of hours.

One of the most relevant testing conditions is MPPT under 1 sun illumination, as it mimics real operating conditions. By plotting the  $T_{80}$ , that is, the time it takes the devices to lose 20% of the initial power output, against publication year for MHPs tested under 1 sun with MPPT (Figure 11B), substantial progress can be noted, both in the number of cells that have undergone those test conditions and in the maximum performance, where we recently have seen  $T_{80}$  values over 1000 h. Looking at the data in further detail reveals that the most stable cells also often have a relatively high efficiency. In part that could be due to an experimental bias of favouring high efficiency devices for time-consuming stability measurements, but it is nevertheless an indication of a positive correlation between high efficiency and stability, which is good news from a technological perspective.

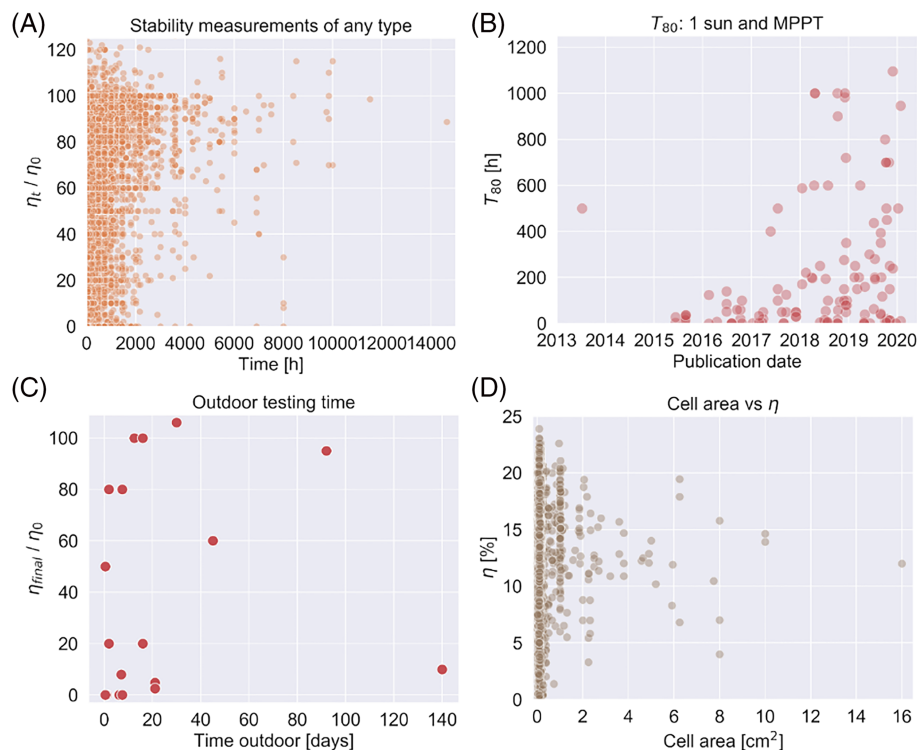


**FIGURE 11** All data are based on the Perovskite Database Project. (A) Relative decrease in performance at the end of the stability measurement versus total exposure time for all samples in the database, regardless of perovskite composition, cell architecture, stack sequence, perovskite composition, initial efficiency and testing condition. (B) T80 values for cells measured under 1 sun and MPPT conditions as a function of publication year. (C) Percentage of initial performance remaining at the end of the stability measurement versus total exposure time for cells measured under outdoor conditions. (D) Efficiency as a function of cell area where a stability measurement has been reported.<sup>168</sup>

Indoor measurements do not necessarily replicate the stress conditions of real world outdoor operational conditions, with seasons, weather, day-night cycles and varying temperature load. To really assess the reliability of perovskite cells, we thus must leave the lab for the outdoor world. That has been done (Figure 11C), but so far there are only a few reports on outdoor testing and the ones that exist describe data for very few cells. Exposure times longer than a month are available in only a few instances. The available data set for outdoor testing is currently too small to draw conclusions about MHP solar cell reliability in the field, but the increased stability seen with indoor testing indicates that within the next few years, we will see an increasing amount of field testing, which will be interesting to follow.

It is worth mentioning that most of the available data are on small area cells. Similar to other PV technologies, the efficiency tends to decrease when the area goes up due to local defects and material non-uniformity (Figure 11D). Technology learning cycles are necessary to decrease the efficiency gap between small and larger areas.

### 3.4.2 | Failure modes and their mitigation

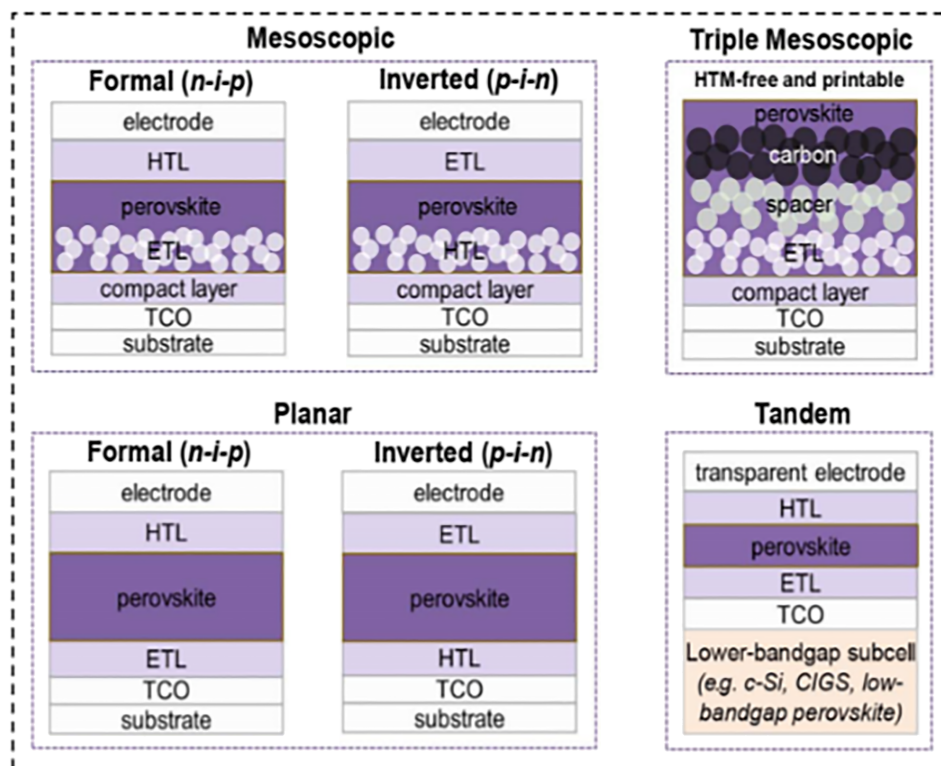
Before discussing about the failure modes of MHP, it is vital to know the structure of MHPs, as this has a bearing on the degradation routes. Typical MHPs consist of at least five layers with four interfaces (see Figure 12). Most MHPs consist of a TCO coated glass substrate as anode or cathode (depending on whether the configuration is *pin* or *nip*, respectively), a perovskite absorber layer, an electron selective *n*-type layer (e.g.  $\text{SnO}_2$ ,  $\text{TiO}_2$  and PCBM) or an hole selective *p*-type layer (e.g. Spiro-OMeTAD, CuSCN and PTAA) and an anode/

cathode (Au, Cu or Ag), which is also dependent on cell architecture. We can sub-divide MHPs into five classes depending on the placement and nature of the charge-transporting layer, namely, the planar *n-i-p* structure, planar *p-i-n* structure, the mesoscopic *n-i-p* structure, mesoscopic *p-i-n* structure and the triple mesoscopic structure (Figure 12).

The absorber and charge transporting materials can degrade either alone or while in contact with other layers. In the case of the absorber layer, the volatile nature of the organic cation, halide segregation and ion accumulation are undesirable processes that speed up the device degradation. Ion migration at different interfaces induces different types of recombination losses in the MHPs. Recently, MHPs using mixed-halide,<sup>169</sup> mixed-cation<sup>170</sup> and mixed 2D perovskite layers gave competitive device performance and stability. To further increase the stability and performance, doping of the perovskite or of the interfacial layer was adopted.<sup>171,172</sup> Due to the issue associated with the intrinsic degradation of  $\text{MAPbI}_3$ , its formadium analogue,  $\text{FAPbI}_3$ , is being now extensively studied as material with a high tolerance factor. However, at room temperature, it acquires a non-perovskite  $\delta$ -phase, which needs to be overcome by additive engineering. In other efforts to increase stability, interfacial modifications were made, and different types of new charge transport materials such as  $\text{BaSnO}_3$ ,<sup>173</sup>  $\text{CuGaO}_2$ ,<sup>174</sup> PTAA<sup>175</sup> and self-assembled layers<sup>176</sup> were explored in *n-i-p* and *p-i-n* configuration.

Several stress factors have been used to identify the failure modes in these MHPs; however, their effect on the device stability is not fully quantified by IEC standards. In the next section, the possible stress factors will be discussed along with the known degradation mechanisms and possible mitigation.

**FIGURE 12** Annotated diagram of a MHP with four device configurations: mesoscopic structure, planar structure, triple mesoscopic structure, and tandem structure with a lower-bandgap subcell. In the mesoporous structure, a thin mesoporous scaffold (typically  $\text{TiO}_2$  or  $\text{Al}_2\text{O}_3$ ) infiltrated with absorber material is present between a charge extraction layer and the polycrystalline absorber layer.<sup>177</sup>



### 3.4.3 | Main stress factors in MHPs

Humidity is one of the main stress factors, owing to the moisture sensitive nature of the organic cation present in hybrid perovskite. The perovskite crystals can be hydrated when in contact with humid air, but this hydration process is reversible. Due to poor thermal stability of the hydrated perovskite, it can however rapidly decompose irreversibly. The presence of light may speed up this degradation. This suggests that investigation of combined stress factors, such as light, temperature and humidity, is paramount, both experimentally and in reliability modelling, to understand the significance of IEC damp heat tests (85°C/85% RH) to predict 25-year operational stability for MHP modules.

#### *Atmosphere composition (moisture and oxygen)*

Perovskite layers are liable to degradation under exposure to moisture and air, to note here moisture, oxygen and UV radiation are indispensable for the degradation process. The mechanism of  $\text{CH}_3\text{NH}_3\text{PbI}_3$  degradation in the presence of  $\text{H}_2\text{O}$  has been studied in a number of papers.<sup>178–180</sup> It leads to the co-existence of the salt with  $\text{PbI}_2$ ,  $\text{CH}_3\text{NH}_3\text{I}$ ,  $\text{CH}_3\text{NH}_2$  and  $\text{HI}$ . The  $\text{HI}$  can be decomposed further into  $\text{H}_2$  and  $\text{I}_2$ . Consuming the  $\text{HI}$  drives the whole decomposition process forward. Similar mechanisms occur in  $\text{FAPbI}_3$ . Both MA, FA and  $\text{HI}$  are volatile at elevated temperatures. Although the bromide (Br) anion-based perovskites are relatively stable, they follow a similar degradation mechanism.

A number of engineering strategies have been adopted in order to improve the stability including interfacial engineering strategies with site-based substitution in the perovskite lattice, doping in charge

transporting layers, passivation by using various materials (small molecules, polymers, ligands, perovskite quantum dots and low-dimensional perovskites) and a protective layer for vulnerable layers.<sup>181</sup> In the recent ‘consensus statement for stability assessment’, it was recommended that testing of devices was still to be conducted under nitrogen environments in order to limit the degradation due to atmospheric factors in order to study other degradation pathways.<sup>182</sup>

#### *Solar visible and UV illumination*

MHPs suffer from photo-induced degradation. The origin is not particularly well understood but likely related to a number of degradation pathways. The mechanism of UV degradation is distinctive under different environments. Although the degradation under illumination at low temperatures in perovskite has shown to be insignificant,<sup>183,184</sup> it increases significantly in the presence of  $\text{H}_2\text{O}$  and  $\text{O}_2$  or in contact with other materials. When MHPs are exposed to light in the presence of oxygen only, the photo-generated electrons react with the  $\text{O}_2$  to form superoxide ( $\text{O}_2^-$ ).<sup>185</sup> This superoxide oxidises the perovskite to  $\text{PbI}_2$ ,  $\text{I}_2$  and  $\text{CH}_3\text{NH}_2^-$  (Figure 13). The  $\text{I}_2$  further oxidises the perovskite. Another unique aspect is that in the absence of  $\text{H}_2\text{O}$  and  $\text{O}_2$ , the degradation of MHPs by UV radiation is partly reversible under 1-sun illumination.<sup>186</sup>

The UV degradation also impacts other layers in the device.<sup>187</sup> Specifically, the most common electron-transport layer,  $\text{TiO}_2$ , is a typical photo-catalyst for oxidising organic materials<sup>188</sup> with a band-gap of 3.20 eV (~400-nm wavelength). It can photocatalyze the decomposition of hybrid perovskite at their interface.<sup>189</sup> The degradation mechanism in the interface of perovskite/ $\text{TiO}_2$  consists of two stages<sup>190</sup> (see again Figure 13). Moreover, charge generation under

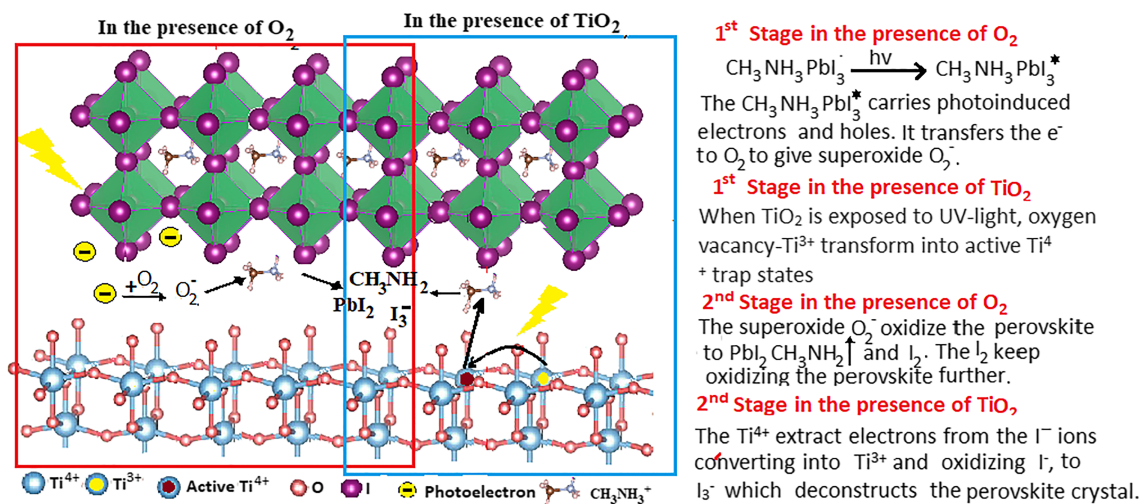


**FIGURE 13** The mechanism of MHP degradation under continuous UV radiation in the presence of  $\text{O}_2$  and/or  $\text{TiO}_2$

light illumination and subsequent trapping on the surface of perovskite has been shown to initiate moisture-induced irreversible degradation to  $\text{PbI}_2$ ,  $\text{CH}_3\text{NH}_2$  and  $\text{HI}$  vapours.<sup>191</sup> Literature reports indicate that the organic cation could become loosely bound to  $\text{PbI}_6^{4-}$  octahedra after light exposure.<sup>192,193</sup>

$\text{TiO}_2$  itself is susceptible to degradation under UV and compromises the durability of MHPs.<sup>194</sup> Increased UV stability with the addition of an additional interlayer ( $\text{Al}_2\text{O}_3$ ,  $\text{Sb}_2\text{S}_3$ ,  $\text{MgO}$  and  $\text{CsBr}$ ) at the perovskite/ $\text{TiO}_2$  interface<sup>183</sup> or replacement of the  $\text{TiO}_2$  layer with another material was reported.<sup>195</sup> The classical hole transporting material (HTM) in the *n-i-p* structure is Spiro-OMeTAD, and it can suffer light induced oxidation alone or in the presence of perovskite.<sup>196</sup> Another reason for the photo-induced degradation in MHPs is the deterioration of the chemical bonding between HTM and Au at the interface, causing insufficient hole extraction.<sup>197</sup> Subsequently, the resistance and carrier recombination increases resulting in degraded PV performance. Formamidinium lead iodide (FAPbI<sub>3</sub>)-based MHPs exhibit better photostability than of  $\text{MAPbI}_3$ <sup>198</sup> and are now being explored.<sup>199</sup>

### Temperature

In the case of MHPs, decomposition can occur during the fabrication process, for example during the annealing of the layers ( $>100^\circ\text{C}$ ) or during high temperature operation. Classical  $\text{MAPbI}_3$ -based MHPs are stable to temperatures up to  $60^\circ\text{C}$ , but at temperatures  $>80^\circ\text{C}$ , the degradation is rapid and irreversible<sup>200</sup> due to its phase transformation as a result of thermal decomposition. By contrast, in the work of Akbulatov et al.,<sup>201</sup> the all-inorganic  $\text{CsPbBr}_3$  displayed no signs of degradation under high temperature and light soaking. Temperature deterioration generally occurs mainly in the bulk of perovskite,<sup>202</sup> but also thermally induced deterioration can take place at the interfaces and in the charge selective layers (HTL or ETL).<sup>64</sup> Different pathways were reported for thermal degradation at variable temperatures.<sup>203</sup>

The thermal degradation of  $\text{CH}_3\text{NH}_3\text{PbI}_3$  can occur even at lower temperatures ( $80^\circ\text{C}$ ) under an inert atmosphere if exposed for

extended time ( $>60$  min),<sup>204</sup> and the decomposition reaction leads to the formation of ammonia ( $\text{NH}_3$ ) and methyl iodide ( $\text{CH}_3\text{I}$ ) gas and lead iodide ( $\text{PbI}_2$ ).<sup>205</sup> It also undergoes a tetragonal-to-cubic phase transition around  $56^\circ\text{C}$ .<sup>203</sup> The structure and PV performance of an operational  $\text{CH}_3\text{NH}_3\text{PbI}_3$ -based planar solar cell was investigated across this phase transition. The device exhibited no significant change in the PV performance parameters ( $J_{\text{SC}}$ ,  $V_{\text{OC}}$  or FF) around the structural phase transition.<sup>206</sup> This indicates an unaffected structure at localised level, where the device's optoelectronics properties are determined.

Besides pure MA and FA-based perovskite, other perovskites with differing compositions of halide anions ( $\text{I}^-$  and  $\text{Br}^-$ ) and organic cations ( $\text{MA}^+$  and  $\text{FA}^+$ ) have been heavily investigated to see the effect of phase transition on thermal stability, device performance and lifetime at  $85^\circ\text{C}$  of solar cells. Compared to pure  $\text{MAPbI}_3$ , perovskite alloys such as  $\text{MA}_{0.6}\text{FA}_{0.4}\text{PbI}_3$ ,  $\text{MAPbI}_{2.6}\text{Br}_{0.4}$  and  $\text{MA}_{0.6}\text{FA}_{0.4}\text{PbI}_{2.8}\text{Br}_{0.2}$  do not show a phase transition in the temperature range from room temperature to  $200^\circ\text{C}$  as measured by differential scanning calorimetry (DSC).<sup>207</sup>  $\text{MA}_{0.6}\text{FA}_{0.4}\text{PbI}_{2.8}\text{Br}_{0.2}$ -based PSCs achieved the best thermal stability due to reduced carrier trap formation as confirmed by thermally stimulated current (TSC) measurements. Moreover, standard ISOS T-1 thermal cycling tests between  $25^\circ\text{C}$  and  $85^\circ\text{C}$  (four cycles) were performed under continuous light irradiation for  $\text{MAPbI}_3$  and  $\text{MA}_{0.6}\text{FA}_{0.4}\text{PbI}_{2.8}\text{Br}_{0.2}$ -based PSCs. In addition, MHPs utilising mixed perovskite absorbers demonstrated reduced degradation behaviour under continuous light irradiation at  $85^\circ\text{C}$  compared to  $\text{MAPbI}_3$ .<sup>208</sup> Electro-chemical impedance spectroscopy (EIS) measurement of fresh and aged PSC under different temperature further proved the influence of the phase transition of  $\text{MAPbI}_3$  on the creation of carrier traps and cause of degradation.<sup>207</sup> These traps are harmful to long-term stability and can be avoided using perovskite alloys with mixed both cations and anions. It is also suggested that at high-temperature, gold diffusion can occur from the electrode through the HTL to the perovskite layer to deteriorate the performance of MHPs,<sup>206</sup> while above  $80^\circ\text{C}$ , large voids are created in the Spiro-OMeTAD layer,<sup>207</sup> and all this compromises reliability. While gold is

unlikely to be used in scalable production, the mechanism of metal diffusion from front and rear electrodes might need further evaluation in the future,<sup>209</sup> as it has also been witnessed in other technologies.

#### Mechanical stability

MHPs exhibit poor resistance to fracture and are considered extremely fragile in the presence of applied loads.<sup>208</sup> The mechanical stability of the MHPs strongly depends on the architecture used and the surrounding layers (HTL, ETL, electrodes, etc). Experiments showed two points of failure for MHPs<sup>210</sup>: firstly, the adhesion of charge-transporting materials to the perovskite layer and secondly, the cohesive failure of these auxiliary charge transporting materials. The perovskite layer itself does not exhibit significant resistance to fracture due to the brittle, salt-like crystal structure. Mechanical stability can be improved by choosing the appropriate architecture, materials and preparation methods. Flexible devices capable of withstanding hundreds of bending cycles<sup>211</sup> have been reported.

#### Charge extraction layers and electrode

The most common electron transport materials in the *n-i-p* structure are based on metal oxides such as TiO<sub>2</sub>, ZnO and SnO<sub>2</sub>. The TiO<sub>2</sub> is the most extensively studied but shows degradation under UV irradiation. Spiro-OMeTAD, the typical HTM, may also degrade by UV. Additionally, the HTL layer may contain pinholes. Through these pinholes, H<sub>2</sub>O and O<sub>2</sub> can permeate and decompose the MA or FA-based perovskite. Meanwhile, mobile ions also migrate from the perovskites and degrade the HTL; see Figure 14.

Furthermore in *n-i-p* architecture, the commonly used metal electrode is gold while for *p-i-n*, silver, copper and aluminium are used. These electrodes can be corroded by I<sub>2</sub> or I<sup>-</sup> that migrates from the perovskite layer through the HTL. The migration of ions towards the electrode is boosted by the presence of humidity due to partial hydrolysis of perovskite. The silver electrodes, although cost-effective when compared to gold, can degrade fast by oxidation or it can react with perovskite to form AgX (X = Cl, Br or I depending on the perovskite used), causing short circuits and degradation of MHPs.<sup>212</sup> Similarly, Al reacts with the I<sub>2</sub> to form AlI<sub>3</sub>. Though Au shows high corrosion resistance to iodine, it can also be corroded in the presence of I<sub>2</sub> and I<sup>-</sup> to form AuI<sub>2</sub> and AuI<sub>3</sub>.<sup>213</sup>

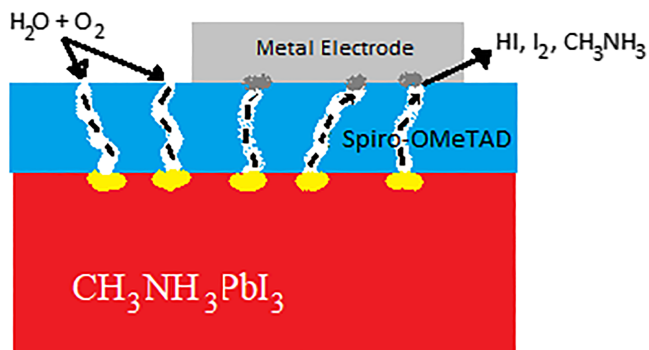


**FIGURE 14** Mechanism of MHP degradation through the pinholes of Spiro-OMeTAD

## 4 | LESSONS LEARNED FROM MATURE AND EMERGING PV TECHNOLOGIES

The approach and contents of the sections for mature (Section 2) versus emerging technologies (Section 3) are very different. The main reason for this can be found in the difference in technology readiness levels (TRLs). While the best literature report for outdoor lifetime for c-Si, CIGS or CdTe modules is bigger than 20 years, outdoor experience for DSC, OPV and MHP is ranging from 0.5 to 2 years<sup>5</sup>. Table 1 has been prepared to highlight the key specific degradation and failure mechanisms for each PV technology in order to provide a summary for the reader. And the presentation in Table 2 makes it clear that Section 2 for the mature technologies focuses more on degradation in the field and thus on the types of degradation caused by external stress. By comparison, by lack of long-term outdoor experience, Section 3 deals mainly with inherent instability problems in emerging technologies.

One of the aims of this review article is to identify lessons learnt from mature technologies in order to aid the development of next generation PV technologies. It is clear for the commercial viability of any PV technology that reliability is key and it should not be separated from other product development aspects. Therefore, also for lab scale PV technologies, it is important to explore how reliability can be optimised already under laboratory conditions.

This section aims to summarise what lessons learnt from mature PV could be transferred to emerging PV. Firstly, the inherent stability of the active materials and components when exposed to light and heat that are unavoidable for any PV technology. Next is the chemical stability of the active materials to external factors, such as water ingress and chemical attack due to ancillary component degradation. Finally, are the external electrical and mechanical factors resultant from deploying the modules in an outdoor environment.

For many new technologies, the module components will be similar to those for mainstream technologies, such as the encapsulation and interconnect materials (e.g. TCO). Therefore, the understanding of these components and their testing approaches can be readily applied to new solar cell materials. However, the sources of instability for new PV technologies are numerous and include intrinsic material properties (e.g. absorber layer and electrode) and extrinsic environmental conditions (humidity, light, temperature, oxygen/water vapour and thermal changes), among others. Like in the early stages of c-Si, CdTe and CIGS technology development, most research on emerging technologies focuses on advancements of the cell technology. In the following, we will address the long-term stability of third generation PV technologies, OPV, DSC and MHP.

### 4.1 | In lab inherent stability

For OPV and DSC, power conversion efficiencies of resp. >18% and 14% have been reported for lab scale devices. It can be argued that if significant advances in the power conversion efficiencies of these

technologies do not occur, then investing resources into understanding intrinsic and extrinsic stability is pointless. It is very difficult to argue for a significant adoption of a PV technology with power conversion efficiencies well below 20%. In the case of liquid electrolyte-based DSC, this limitation arises from the large voltage losses required to efficiently drive charge separation and also from the limited absorption spectra of the dyes. Theoretically, achievable efficiencies in solid-state DSC are higher, and the configuration in solid state suggests improved stability.

Perovskite-based solar cells are, however, extremely promising. Their power conversion efficiencies have surged at an unprecedented pace for a PV technology. In the last decade, operational stabilities of such devices have risen from minutes to months, and if that development continues, perovskite-based PVs may soon become a contender in the field. The recent developments in the device architecture, compositional engineering, rational charge selective materials, additives and so on can pave the way for production with long lifetime. In addition, mature technologies such as silicon became very reliable once the process was more fully developed. For example, the reduction in sodium and potassium by cleanroom processing and the surface passivation to reduce recombination rates had a major effect. Additionally, the encapsulation processes were optimised, which removed damage due to water ingress and mechanical loading. So, modules or mini-modules should be used for ageing tests to identify module level failure mechanisms in order to design possible mitigation steps. The maturation of this technology is reflected by the fact the community has devised standard testing protocols. In this direction, a close collaboration of inter-laboratory device testing will be of significant importance to understand and resolve the degradation mechanisms.

Aside from module packaging, which is similar between c-Si and thin film, the mature thin film technologies (CdTe, CIGS) provide more lessons for emerging technologies. Any cell degradation modes commonly found in thin film cells (such as pinholes, reverse bias, shunting, TCO corrosion) would be the main topics of concern for an emerging thin film PV technology.

## 4.2 | Passive components, packaging and ancillaries

Many degradation and failure modes are related to module components other than the solar cells. In particular, the polymeric materials used as encapsulants and backsheets can play a significant role in cell and module degradation. Their molecular degradation products can interact with other module components, for example EVA generates acetic acid that among other effects corrodes cells and metallisation. Because they are permeable, the polymers also determine the availability of water vapour and oxygen in PV modules. Thus, the Balance of Materials (BOM) of any emerging technology should be carefully selected, considering possible degradation products, permeation properties and possible incompatibilities.

## 4.3 | Field testing

Understanding why failures happen is key for improvement in reliability. A detailed understanding of the various failure modes occurring during in-field operation of the solar cells is required to minimise or eliminating performance losses. Failure modes and effects analysis (FMEA) should be used to grow module reliability. An objective approach to improvement is required, where researchers apply strong test programmes with measurements of all failure modes, which can be used to assess actual failure obtained from accelerated and outdoor testing. Key to this will be the material/root cause failure analysis that in some cases needs operando techniques to decipher the kinetics.

## 4.4 | Accelerated lifetime testing (ALT)

Together with field tests, ALT is of fundamental importance to reduce the time to market for a new PV technology. Ideally, this requires thorough understanding that ALT testing is reproducing only the failure modes observed under real operational conditions. While indoor stability studies are more prevalent in the literature, outdoor tests provide an opportunity to understand material and device degradation under field conditions. Furthermore, outdoor studies from the whole PV community show that failure modes are either reduced or increased in severity under outdoor conditions and even that different failure modes are observed outdoors, which are not observed from indoor ALT tests.

The case of OPV and DSC has highlighted that standards issued by the International Electrotechnical Commission can overstress the devices leading to failure modes that do not necessarily occur in the field. Therefore, technology-specific tests are required to properly estimate the potential failure rates in emerging PV technologies. Most studies on perovskite stability to date have been focused on considering one or two stresses and/or the alteration of materials for improved intrinsic stability. Although a stability study under one applied stress can provide meaningful information, it does not provide information about the likely outdoor stability where multiple stresses are simultaneously applied. Multi-stress is a good methodology to ensure acceleration factors remain high, without overstressing the device. Other PV technologies can no longer rely on just the main module qualification standards (IEC 61215, IEC 61730). It is worth pointing out that it is possible to modify, expand or add tests to IEC standards to address new failure modes.

## 4.5 | Extrapolating from in lab stability test to in field stability

Standard High Temp/humidity/light ALT simply does not stimulate the types of complex material systems found in 3rd generation technologies with organic layers, hybrid barrier layers, sealing layers and so on. One of the impediments for undertaking both outdoor testing

and ALT of new PV materials has been the issue of scalability. Specifically, transferring knowledge gained about performance from tests on a small device or single material or component to a complete system (module). For example, meta-analysis by the authors shows that from 500 research papers on perovskites published between 2017 and 2019, the vast majority of devices reported on were small sized laboratory scale devices with >94% having an active area of 0.2cm<sup>2</sup> or less. There is no straightforward means of linking performance of small-scale devices to that of full-size modules, and as devices get larger, the higher sheet resistivity of the transparent electrode (typically ITO or FTO) leads to increased series resistance. With the scaling of devices, quality control becomes more important and fundamental changes to processing factors such as solvents, solution formulations, material selection and device design have to be made, all that are likely to influence the stability of the final product and limit the usefulness of small-scale stability tests. Conversely, scaling from cells to modules, edge effects become less significant.

#### 4.6 | Module external stress factor effects

Certain stress factors are not well studied in emerging PV, such as soiling, chemical pollutants and, to some extent, mechanical loading. The latter is particularly interesting; next generation PVs modules are often on flexible substrates so the types of mechanical stress are different to one would expect from a mature module. While it is commonplace to see tests on repeated bending, prolonged flexing under load such as wind might trigger a different failure mechanism. Indeed, the mounting format is likely to play a role in the mechanical stability. Longer-term soiling and chemical pollution might have an influence. The mismatch in thermal expansion coefficients and low fracture energy of layers in MHPs raise a concern as to whether devices can withstand mechanical stresses from temperature fluctuations. Large mismatches in CTE between adjacent materials could build up stress and lead to delamination during temperature cycling, which presents a direct path for moisture ingress to the solar cells. In addition, the metal oxide barrier layers used with flexible substrates might degrade under sustained chemical pollutant exposure.

Encapsulants need to be chosen carefully to be optically transparent, flexible enough to absorb any fluctuation in strain energy during temperature cycling, electrically insulating to mitigate PID, to have a reasonably low water vapour transmission rate and to not release by-products that would be harmful to the electrical contacts and solar cell absorber (e.g. acetic acid and EVA).

One specific challenge faced with next generation modules is the high voltage when large numbers of cells are connected in series, leading potentially to PID issues or arcing. As an example, a 2.1-m-long perovskite solar cell module with 1-cm-wide serially connected cells would have an open circuit voltage of around 184 V,<sup>214</sup> compared to around 46 V for a same sized c-Si module. Clearly, ensuring these higher operating voltages do not have an impact if the substrates are thin films is a vital research area. Another critical aspect is shear forces that build up in molten or liquid encapsulants during module

production, which eventually could break the absorber materials. Stability of the encapsulants and edge sealants (if applicable) is required to minimise this. There is very little work in next generation PVs on edge sealants, and this is also an area that needs more research.

By simply considering internal stability issues of next generation technologies, it is clear that major improvements in encapsulation and module packaging are required. Many encapsulation strategies in literature are at low TRLs or too expensive for scalable use. Moving production to scale will add quality-engineering issues that are presently unknown; the EVA issues stipulated in Section 2.1.2 show how a stable material can give problems as companies move to mass manufacture. As the drive to low cost, mass manufacture starts for emerging technologies, issues with packaging will become more commonplace.

## 5 | CONCLUSION

The aim of the review paper was to describe technology specific degradation modes of the different PV technologies. The paper not just introduced degradation modes found in mature PV technologies (c-Si, CdTe and CIGS) but also provided a review of known failure modes and areas of future research for emerging technologies such as DSCs, organic PV and perovskite solar cells. The review paper discussed known failure mechanisms and developmental issues that were discovered in mature and commercially available PV technologies and how they might impact emerging PV technologies. It is hoped that lessons learnt from mature technologies might speed up development of these emerging technologies.

Degradation modes typical for c-Si PV are cell cracks, snail trails and hot spots as well as PID, LID and LETID. PID is also found in CdTe and CIGS modules. Especially, CIGS modules are also sensitive to partial shading and water ingress. Partial shading can result in the non-reversible formation of wormlike defects. In these defects, the CIGS absorber material has recrystallised and formed into a thick semi-porous and likely conductive structure. Water ingress decreases the conductivity of the TCO front contact. For CdTe modules, the mechanism appears to be related to sodium ion diffusion into the cell. CdTe differs from CIGS in that it is superstrate configuration where the films are deposited directly onto a TCO coated soda lime glass. However, the PID can be reversed by applying a reverse bias, provided the modules are operated in a dry environment.

The review made it clear that the long-term stability of third generation PV technologies (OPV, DSC, MHP) remains a challenge and needs to be addressed for achieving rapid commercialisation. These technologies replace inorganic materials by organic materials where possible and adopt roll-to-roll fabrication techniques. However, even though the use of organic materials induces opportunities for tuning of functional properties, it also introduces numerous degradation and scale-up issues. Firstly, unlike the mature solar cell technologies, the organic absorber components are, themselves, prone to oxidation. Additionally, material compatibility and unintended side reactions of electrode, absorber and interlayer materials are a big challenge for emerging cell technologies.

Like in the early stages of c-Si, CdTe and CIGS technology development, most research on emerging technologies focuses on advancements of the cell technology. However, many degradation and failure modes are related to other module components and not the solar cells. In particular, the module packaging can play a significant role in cell and module degradation, so the BOM of any emerging technology should be carefully selected, considering permeation properties and possible incompatibilities.

Aside from module packaging, which is similar between c-Si and thin film, the mature thin film technologies (CdTe, CIGS) most probably will provide more lessons for emerging technologies. Understanding the long-term materials processes such as dopant or impurity diffusion will be common to all thin film technologies. In the case of CdTe, degradation associated with diffusion of the commonly used copper dopant is seen. Replacing copper with the much slower diffusing arsenic dopant has shown significantly reduced degradation. Any cell degradation modes commonly found in thin film cells (such as pinholes, reverse bias, shunting, TCO corrosion) would be the main topics of concern for an emerging thin film PV technology.

Understanding why failures happen is key for improvement in reliability. A detailed understanding of the various failure modes occurring during in-field operation of the solar cells is key to minimising or eliminating performance losses. One of the impediments for understanding the long-term behaviour of emerging solar cell technologies has been the issue of scalability. The vast majority of disseminated MHP devices were small sized laboratory scale devices with >94% having an active area of 0.2 cm<sup>2</sup> or less. There is no straightforward means of linking performance of small-scale devices to that of full-size modules, especially as edge effects become less significant. Also, certain stress factors are not well studied in emerging PV, such as soiling, chemical pollutants and, to some extent, mechanical loading. The latter is particularly interesting as next generation PVs modules are often on flexible substrates, and there, a different mechanical stress distribution is to be expected.

Summarised, it is clear for the commercial viability of any PV technology that reliability is key, and it should not be separated from upscaling and other product development aspects. Therefore, especially for emerging lab scale PV technologies, it is important to explore how reliability can be optimised already under laboratory conditions.

## ACKNOWLEDGEMENT

This review article is based upon work from COST Action CA16235 PEARL PV, WG2, supported by COST (European Cooperation in Science and Technology), a funding agency for research and innovation networks.

## DATA AVAILABILITY STATEMENT

Data sharing is not applicable to this article as no new data were created or analyzed in this study.

## ORCID

Jeff Kettle  <https://orcid.org/0000-0002-1245-5286>

Mohammadreza Aghaei  <https://orcid.org/0000-0001-5735-3825>

Andrew Fairbrother  <https://orcid.org/0000-0001-6038-7532>

Stuart Irvine  <https://orcid.org/0000-0002-1652-4496>

Dan Lamb  <https://orcid.org/0000-0002-4762-4641>

Killian Lobato  <https://orcid.org/0000-0002-1002-9363>

Georgios A. Mousdis  <https://orcid.org/0000-0002-0560-4829>

Gernot Oreski  <https://orcid.org/0000-0003-4223-9047>

Angele Reinders  <https://orcid.org/0000-0002-5296-8027>

Jurriaan Schmitz  <https://orcid.org/0000-0002-9677-825X>

Mirjam J. Theelen  <https://orcid.org/0000-0002-3864-1933>

## REFERENCES

1. Atsu D, Seres I, Aghaei M, Farkas I. Analysis of long-term performance and reliability of PV modules under tropical climatic conditions in sub-Saharan. *Renew Energy*. 2020;162:285-295. doi:10.1016/j.renene.2020.08.021
2. Annigoni E, Virtuani A, Caccivio M, Friesen G, Chianese D, Ballif C. 35 years of photovoltaics: Analysis of the TISO-10-kW solar plant, lessons learnt in safety and performance—part 2. *Prog Photovoltaics Res Appl*. 2019;27(9):760-778. doi:10.1002/pip.3146
3. SunPower Corporation. SunPower Module: 40-Year Useful Life. *White Pap*. 2013;99:1-20.
4. Santhakumari M, Sagar N. A review of the environmental factors degrading the performance of silicon wafer-based photovoltaic modules: failure detection methods and essential mitigation techniques. *Renew Sustain Energy Rev*. 2019;110:83-100. doi:10.1016/j.rser.2019.04.024
5. Aghaei M, Fairbrother A, Gok A, et al. Review of degradation and failure phenomena in photovoltaic modules. *Renew Sustain Energy Rev*. 2022;159:112160. doi:10.1016/j.rser.2022.112160
6. El Chaar L, Lamont LA, El Zein N. Review of photovoltaic technologies. *Renew Sustain Energy Rev*. 2011;15(5):2165-2175. doi:10.1016/j.rser.2011.01.004
7. Munoz MA, Alonso-García MC, Vela N, Chenlo F. Early degradation of silicon PV modules and guaranty conditions. *Sol Energy*. 2011; 85(9):2264-2274. doi:10.1016/j.solener.2011.06.011
8. Sharma V, Chandel SS. A novel study for determining early life degradation of multi-crystalline-silicon photovoltaic modules observed in western Himalayan Indian climatic conditions. *Sol Energy*. 2016; 134:32-44. doi:10.1016/j.solener.2016.04.023
9. Ndiaye A, Charki A, Kobi A, Kébé CMF, Ndiaye PA, Sambou V. Degradations of silicon photovoltaic modules: A literature review. *Sol Energy*. 2013;96:140-151. doi:10.1016/j.solener.2013.07.005
10. Ndiaye A, Kébé CMF, Charki A, Ndiaye PA, Sambou V, Kobi A. Degradation evaluation of crystalline-silicon photovoltaic modules after a few operation years in a tropical environment. *Sol Energy*. 2014; 103:70-77. doi:10.1016/j.solener.2014.02.006
11. Sinha A, Qian J, Hurst K, et al. UV-Induced degradation of high-efficiency solar cells with different architectures. In *2020 47th IEEE Photovoltaic Specialists Conference (PVSC) 1990-1991* (IEEE, 2020).
12. Sinha A, Hurst K, Uličná S, et al. Assessing UV-induced degradation in bifacial modules of different cell technologies. In *2021 IEEE 48th Photovoltaic Specialists Conference (PVSC) 767-770* (IEEE, 2021).
13. ITRPV. *International Technology Roadmap for Photovoltaic (ITRPV)*. Ninted, 2018 results. *Itrpv*; 2018. VDMA GmbH.
14. Köntges M, Siebert M, Morlier A, Illing R, Bessing N, Wegert F. Impact of transportation on silicon wafer-based photovoltaic modules. *Prog Photovoltaics Res Appl*. 2016;24(8):1085-1095. doi:10.1002/pip.2768
15. Assmus M, Jack S, Weiss KA, Koehl M. Measurement and simulation of vibrations of PV-modules induced by dynamic mechanical loads. *Prog Photovoltaics Res Appl*. 2011;19(6):688-694. doi:10.1002/pip.1087

16. Camus C, Adegbenro A, Ermer J, Suryaprakash V, Hauch J, Brabec CJ. Influence of pre-existing damages on the degradation behavior of crystalline silicon photovoltaic modules. *J Renew Sustain Energy*. 2018;10(2):21004. doi:10.1063/1.5000294
17. Buerhop C, Wirsching S, Bemm A, et al. Evolution of cell cracks in PV-modules under field and laboratory conditions. *Prog Photovoltaics Res Appl*. 2018;26(4):261-272. doi:10.1002/pip.2975
18. Kilikevičienė K, Matijošius J, Kilikevičius A, et al. Research of the energy losses of photovoltaic (PV) modules after hail simulation using a newly-created testbed. *Energies*. 2019;12(23):4537. doi:10.3390/en12234537
19. Gou X, Li X, Wang S, Zhuang H, Huang X, Jiang L. The effect of microcrack length in silicon cells on the potential induced degradation behavior. *Int J Photoenergy*. 2018;2018:1-6. doi:10.1155/2018/4381579
20. Papargyri L, Theristis M, Kubicek B, et al. Modelling and experimental investigations of microcracks in crystalline silicon photovoltaics: a review. *Renew Energy*. 2020;145:2387-2408. doi:10.1016/j.renene.2019.07.138
21. Kntges M, Kunze I, Kajari-Schrder S, Breitenmoser X, Bjørneklett B. The risk of power loss in crystalline silicon based photovoltaic modules due to micro-cracks. *Sol Energy Mater Sol Cells*. 2011;95(4):1131-1137. doi:10.1016/j.solmat.2010.10.034
22. Spataru S, Cernek P, Sera D, Kerekes T, Teodorescu R. Characterization of a crystalline silicon photovoltaic system after 15 years of operation in Northern Denmark. In *29th European Photovoltaic Solar Energy Conference and Exhibition*; 2014. doi:10.4229/EUPVSEC20142014-5BV.1.31
23. Dhimish M, Kettle J. Impact of solar cell cracks caused during potential-induced degradation (PID) tests. *IEEE Trans Electron Devices*. 2021;69(2):604-612. doi:10.1109/TED.2021.3135365
24. Abdelhamid M, Singh R, Omar M. Review of microcrack detection techniques for silicon solar cells. *IEEE Journal of Photovoltaics*. 2014;4(1):514-524. doi:10.1109/JPHOTOV.2013.2285622
25. Anwar SA, Abdullah MZ. Micro-crack detection of multicrystalline solar cells featuring an improved anisotropic diffusion filter and image segmentation technique. *Eurasip J Image Video Process*. 2014;15. doi:10.1186/1687-5281-2014-15
26. Pérez R, Gumbsch P. Ab initio study of the cleavage anisotropy in silicon. *Acta Mater*. 2000;48(18-19):4517-4530. doi:10.1016/S1359-6454(00)00238-X
27. Wen TK, Yin CC. Crack detection in photovoltaic cells by interferometric analysis of electronic speckle patterns. *Sol Energy Mater Sol Cells*. 2012;98:216-223. doi:10.1016/j.solmat.2011.10.034
28. Schulze K, Groh M, Nieß M, et al. Untersuchung von Alterungseffekten bei monokristallinen PV-Modulen mit mehr als 15 Betriebsjahren durch Elektrolumineszenz- und Leistungsmessung. In *Proc. 28. Symposium Photovoltaische Solarenergie*; 2012.
29. Khatri R, Agarwal S, Saha I, Singh SK, Kumar B. Study on long term reliability of photo-voltaic modules and analysis of power degradation using accelerated aging tests and electroluminescence technique. *Energy Procedia*. 2011;8:396-401. doi:10.1016/j.egypro.2011.06.156
30. Chaturvedi P, Hoex B, Walsh TM. Broken metal fingers in silicon wafer solar cells and PV modules. *Solar Energy Materials and Solar Cells*. 2013;108:78-81. doi:10.1016/j.solmat.2012.09.013
31. Meyer S, Timmel S, Gläser M, Braun U, Wachtendorf V, Hagedorf C. Polymer foil additives trigger the formation of snail trails in photovoltaic modules. *Sol Energy Mater sol Cells*. 2014;130:64-70. doi:10.1016/j.solmat.2014.06.028
32. Grimaccia F, Leva S, Dolara A, Aghaei M. Survey on PV Modules' Common Faults After an O&M Flight Extension Campaign Over Different Plants in Italy. *IEEE J Photovoltaics*. 2017;7(3):810-816. doi:10.1109/JPHOTOV.2017.2674977
33. Meyer S, Richter S, Timmel S, et al. Snail trails: root cause analysis and test procedures. *Energy Procedia*. 2013;38:498-505. doi:10.1016/j.egypro.2013.07.309
34. Köntges M, Kurtz S, Packard CE, et al. Review of failures of photovoltaic modules. *IEA-Photovoltaic Power Systems Programme*. 2014;1-140. doi:978-3-906042-16-9
35. Fan J, Ju D, Yao X, et al. Study on snail trail formation in PV module through modeling and accelerated aging tests. *Sol Energy Mater Sol Cells*. 2017;164:80-86. doi:10.1016/j.solmat.2017.02.013
36. He W, Yang J, Lei L, et al. Long term testing over 6 years on crystalline silicon solar modules with snail trails. In *2018 IEEE 7th World Conference on Photovoltaic Energy Conversion, WCPEC 2018 - A Joint Conference of 45th IEEE PVSC, 28th PVSEC and 34th EU PVSEC*; 2018. doi:10.1109/PVSC.2018.8547896
37. Quater PB, Grimaccia F, Leva S, Mussetta M, Aghaei M. Light Unmanned aerial vehicles (UAVs) for cooperative inspection of PV plants. *IEEE J Photovoltaics*. 2014;4(4):1107-1113. doi:10.1109/JPHOTOV.2014.2323714
38. Dolara A, Leva S, Manzolini G, Ogliari E. Investigation on performance decay on photovoltaic modules: Snail trails and cell micro-cracks. *IEEE J Photovoltaics*. 2014;4(5):1204-1211. doi:10.1109/JPHOTOV.2014.2330495
39. Yang H, He W, Wang H, Huang J, Zhang J. Assessing power degradation and reliability of crystalline silicon solar modules with snail trails. *Sol Energy Mater sol Cells*. 2018;187:61-68. doi:10.1016/j.solmat.2018.07.021
40. Bristow N, Kettle J. Outdoor organic photovoltaic module characteristics: benchmarking against other PV technologies for performance, calculation of Ross coefficient and outdoor stability monitoring. *Sol Energy Mater Sol Cells*. 2018;175:52-59. doi:10.1016/j.solmat.2017.10.008
41. Moradi AM, Aghaei M, Esmailifar SM. A deep convolutional encoder-decoder architecture for autonomous fault detection of PV plants using multi-copters solar energy. *Sol Energy*. 2021;223:217-228. doi:10.1016/j.solener.2021.05.029
42. Aghaei M, Gandelli A, Grimaccia F, Leva S, Zich RE. IR real-Time analyses for PV system monitoring by digital image processing techniques. In *Proceedings of 1st International Conference on Event-Based Control, Communication and Signal Processing, EBCCSP 2015*; 2015. doi:10.1109/EBCCSP.2015.7300708
43. Molenbroek E, Waddington DW, Emery KA. Hot spot susceptibility and testing of PV modules. In *Conference Record of the IEEE Photovoltaic Specialists Conference*; 1992. doi:10.1109/pvsc.1991.169273
44. Eskandari A, Milimonfared J, Aghaei M. Line-line fault detection and classification for photovoltaic systems using ensemble learning model based on i-v characteristics. *Sol Energy*. 2020;211:354-365. doi:10.1016/j.solener.2020.09.071
45. Eskandari A, Milimonfared J, Aghaei M, Oliveira AK, Rütther R. Line-to-line faults detection for photovoltaic arrays based on I-V curve using pattern recognition. In *IEEE 46th Photovoltaic Specialists Conference (PVSC)*; 2019.
46. Aghaei M. Novel methods in control and monitoring of photovoltaic systems. (PhD Thesis, Politecnico di Milano); 2016.
47. de Oliveira AKV, Aghaei M, Rütther R. Automatic inspection of photovoltaic power plants using aerial infrared thermography: a review. *Energies*. 2022;15(6):2055. doi:10.3390/en15062055
48. Eskandari A, Milimonfared J, Aghaei M. Fault detection and classification for photovoltaic systems based on hierarchical classification and machine learning technique. *IEEE Trans Ind Electron*. 2020;68(12):12750-12759. doi:10.1109/TIE.2020.3047066
49. Sharma V, Sastry OS, Kumar A, Bora B, Chandel SS. Degradation analysis of a-Si, (HIT) hetero-junction intrinsic thin layer silicon and m-C-Si solar photovoltaic technologies under outdoor conditions. *Energy*. 2014;72:536-546. doi:10.1016/j.energy.2014.05.078

50. Wendlandt S, Drobisch A, Tornow D, et al. Operating principle of shadowed C-Si solar cell in PV-modules. In *30th ISES Biennial Solar World Congress 2011, SWC 2011*; 2011. doi:[10.18086/swc.2011.14.18](https://doi.org/10.18086/swc.2011.14.18)
51. Leva S, Aghaei M. Failures and defects in PV Systems. *Power Eng Adv Challenges Part B Electr Power*. 2018;55:56-84.
52. Dhimish M, Tyrrell AM. Power loss and hotspot analysis for photovoltaic modules affected by potential induced degradation. *Npj Mater Degrad*. 2022;6(1):1-8. doi:[10.1038/s41529-022-00221-9](https://doi.org/10.1038/s41529-022-00221-9)
53. Aghaei M, Madukanya UE, Kirsten A, De Oliveira V. Fault inspection by aerial infrared thermography in a PV plant fault inspection by aerial infrared thermography in a. *VII Congr. Bras Energ sol - CBENS 2018*; 2018.
54. De Oliveira AKV, Aghaei M, Madukanya UE, Nascimento L, Ruther R. Aerial infrared thermography of a utility-scale PV plant after a meteorological tsunami in Brazil. *2018 IEEE 7th World Conf. Photovolt. Energy Conversion, WCPEC 2018 - A Jt. Conf. 45th IEEE PVSC, 28th PVSEC 34th EU PVSEC 1*; 2018: 684-689.
55. Oh W, Bae S, Chan SI, Lee HS, Kim D, Park N. Field degradation prediction of potential induced degradation of the crystalline silicon photovoltaic modules based on accelerated test and climatic data. *Microelectron Reliab*. 2017;76:596-600. doi:[10.1016/j.microrel.2017.07.079](https://doi.org/10.1016/j.microrel.2017.07.079)
56. Naumann V, Lausch D, Hähnel A, et al. Explanation of potential-induced degradation of the shunting type by Na decoration of stacking faults in Si solar cells. *Sol Energy Mater Sol Cells*. 2014;120:383-389. doi:[10.1016/j.solmat.2013.06.015](https://doi.org/10.1016/j.solmat.2013.06.015)
57. Swanson R, Cudzinovic M, DeCeuster D, et al. The Surface polarization effect in high-efficiency silicon solar cells. *15th International PVSEC*; 2005:4-7.
58. Sporleder K, Naumann V, Bauer J, et al. Local corrosion of silicon as root cause for potential-induced degradation at the rear side of bifacial PERC solar cells. *Phys Status Solidi (RRL)-Rapid Res Lett*. 2019; 13(9):1900163. doi:[10.1002/pssr.201900163](https://doi.org/10.1002/pssr.201900163)
59. Sporleder K, Naumann V, Bauer J, et al. Root cause analysis on corrosive potential-induced degradation effects at the rear side of bifacial silicon PERC solar cells. *Sol Energy Mater Sol Cells*. 2019;201: 110062.
60. Fillet R, Nicolas V, Fierro V, Celzard A. A review of natural materials for solar evaporation. *Sol Energy Mater Sol Cells*. 2021;219:110814. doi:[10.1016/j.solmat.2020.110814](https://doi.org/10.1016/j.solmat.2020.110814)
61. Fertig F, Lantzsch R, Mohr A, et al. Mass production of p-type Cz silicon solar cells approaching average stable conversion efficiencies of 22%. *Solar Procedia*. 2017;124:338-345. doi:[10.1016/j.egypro.2017.09.308](https://doi.org/10.1016/j.egypro.2017.09.308)
62. Hallam B, Herguth A, Hamer P, et al. Eliminating light-induced degradation in commercial p-type Czochralski silicon solar cells. *Appl Sci*. 2018;8(1):10. doi:[10.3390/app8010010](https://doi.org/10.3390/app8010010)
63. Kersten F, Engelhart P, Ploigt HC, et al. Degradation of multicrystalline silicon solar cells and modules after illumination at elevated temperature. *Sol Energy Mater Sol Cells*. 2015;142:83-86. doi:[10.1016/j.solmat.2015.06.015](https://doi.org/10.1016/j.solmat.2015.06.015)
64. Chen D, Hamer P, Kim M, et al. Hydrogen-induced degradation: Explaining the mechanism behind light- and elevated temperature-induced degradation in n- and p-type silicon. *Sol Energy Mater Sol Cells*. 2020;207:110353. doi:[10.1016/j.solmat.2019.110353](https://doi.org/10.1016/j.solmat.2019.110353)
65. Witteck R, Min B, Schulte-Huxel H, et al. UV radiation hardness of photovoltaic modules featuring crystalline Si solar cells with AlOx/p+-type Si and SiNy/n+-type Si interfaces. *Phys Status Solidi (RRL)-Rapid Res Lett*. 2017;11(8):1700178. doi:[10.1002/pssr.201700178](https://doi.org/10.1002/pssr.201700178)
66. Vidal K, de Oliveira A, Aghaei M, Ruther R. Aerial infrared thermography for low-cost and fast fault detection in utility-scale PV power plants. *Sol Energy*. 2020;211:712-724. doi:[10.1016/j.solener.2020.09.066](https://doi.org/10.1016/j.solener.2020.09.066)
67. Vidal de Oliveira AK, Amstad D, Madukanya UE, et al. Aerial infrared thermography of a CdTe utility-scale PV power plant. In *2019 IEEE 46th Photovoltaic Specialists Conference (PVSC)*; 2019. doi:[10.1109/PVSC40753.2019.8980575](https://doi.org/10.1109/PVSC40753.2019.8980575)
68. Perrenoud J, Kranz L, Gretener C, et al. A comprehensive picture of Cu doping in CdTe solar cells. *J Appl Phys*. 2013;114(17):174505. doi:[10.1063/1.4828484](https://doi.org/10.1063/1.4828484)
69. Artegiani E, Major JD, Shiel H, Dhanak V, Ferrari C, Romeo A. How the amount of copper influences the formation and stability of defects in CdTe solar cells. *Sol Energy Mater Sol Cells*. 2020;204: 110228. doi:[10.1016/j.solmat.2019.110228](https://doi.org/10.1016/j.solmat.2019.110228)
70. Strevel N, Trippel L, Gloeckler M. Performance characterization and superior energy yield of First Solar PV power plants in high-temperature conditions. *PV Int*. 2012;17:1-8.
71. Bertoncello M, Barbato M, Meneghini M, Artegiani E, Romeo A, Meneghesso G. Reliability investigation on CdTe solar cells submitted to short-term thermal stress. *Microelectron Reliab*. 2019; 100-101:113490.
72. Rugen-Hankey SL, Clayton AJ, Barrioz V, et al. Improvement to thin film CdTe solar cells with controlled back surface oxidation. *Sol Energy Mater Sol Cells*. 2015;136:213-217. doi:[10.1016/j.solmat.2014.10.044](https://doi.org/10.1016/j.solmat.2014.10.044)
73. Metzger WK, Grover S, Lu D, et al. Exceeding 20% efficiency with in situ group V doping in polycrystalline CdTe solar cells. *Nat Energy*. 2019;4(10):837-845. doi:[10.1038/s41560-019-0446-7](https://doi.org/10.1038/s41560-019-0446-7)
74. Kartopu G, Oklobia O, Turkey D, et al. Study of thin film polycrystalline CdTe solar cells presenting high acceptor concentrations achieved by in-situ arsenic doping. *Sol Energy Mater Sol Cells*. 2019; 194:259-267. doi:[10.1016/j.solmat.2019.02.025](https://doi.org/10.1016/j.solmat.2019.02.025)
75. Weber T, Hinz C, Leers M, Grunow P, Podlowski L. A review of potential induced degradation in thin-film plants. *33rd Eur Photovolt Conf Exhib*; 2017. doi:[10.4229/EUPVSEC20172017-5BV.4.59](https://doi.org/10.4229/EUPVSEC20172017-5BV.4.59)
76. Hacke P, Terwilliger K, Glick SH, et al. Survey of potential-induced degradation in thin-film modules. *J Photonics Energy*. 2015;5(1): 053083. doi:[10.1117/1.JPE.5.053083](https://doi.org/10.1117/1.JPE.5.053083)
77. Feurer T, Reinhard P, Avancini E, et al. Progress in thin film CIGS photovoltaics-Research and development, manufacturing, and applications. *Prog Photovoltaics Res Appl*. 2017;25(7):645-667. doi:[10.1002/pip.2811](https://doi.org/10.1002/pip.2811)
78. Jordan DC, Kurtz SR, VanSant K, Newmiller J. Compendium of photovoltaic degradation rates. *Prog Photovoltaics Res Appl*. 2016; 24:978-989.
79. Wennerberg J, Kessler J, Stolt L. Degradation Mechanisms of CIGS based thin film PV modules. *proc. 16th EUPVSEC*; 2000: 309-312.
80. Theelen M, Daume F. Stability of Cu(In,Ga)Se<sub>2</sub> solar cells: A literature review. *Sol Energy*. 2016;133:586-627. doi:[10.1016/j.solener.2016.04.010](https://doi.org/10.1016/j.solener.2016.04.010)
81. Theelen M, Boumans T, Stegeman F, et al. Physical and chemical degradation behavior of sputtered aluminum doped zinc oxide layers for Cu(In,Ga)Se<sub>2</sub> solar cells. *Thin Solid Films*. 2014;550:530-540. doi:[10.1016/j.tsf.2013.10.149](https://doi.org/10.1016/j.tsf.2013.10.149)
82. Theelen M, Dasgupta S, Vroon Z, et al. Influence of the atmospheric species water, oxygen, nitrogen and carbon dioxide on the degradation of aluminum doped zinc oxide layers. *Thin Solid Films*. 2014;565: 149-154. doi:[10.1016/j.tsf.2014.07.005](https://doi.org/10.1016/j.tsf.2014.07.005)
83. Theelen M, Polman K, Tomassini M, et al. Influence of deposition pressure and selenisation on damp heat degradation of the Cu(In,Ga) Se<sub>2</sub> back contact molybdenum. *Surf Coat Technol*. 2014;252: 157-167. doi:[10.1016/j.surfcoat.2014.05.001](https://doi.org/10.1016/j.surfcoat.2014.05.001)
84. Malmström J, Wennerberg J, Stolt L. A study of the influence of the Ga content on the long-term stability of Cu(In,Ga)Se<sub>2</sub> thin film solar cells. *Thin Solid Films*. 2003;431-432:436-442. doi:[10.1016/S0040-6090\(03\)00185-8](https://doi.org/10.1016/S0040-6090(03)00185-8)
85. Kim JI, Lee W, Hwang T, et al. Quantitative analyses of damp-heat-induced degradation in transparent conducting oxides. *Sol Energy*

- Mater Sol Cells*. 2014;122:282-286. doi:[10.1016/j.solmat.2013.12.014](https://doi.org/10.1016/j.solmat.2013.12.014)
86. Steinhäuser J, Meyer S, Schwab M, et al. Humid environment stability of low pressure chemical vapor deposited boron doped zinc oxide used as transparent electrodes in thin film silicon solar cells. *Thin Solid Films*. 2011;520:558-562. doi:[10.1016/j.tsf.2011.06.095](https://doi.org/10.1016/j.tsf.2011.06.095)
  87. Tohsophon T, Hüpkes J, Calnan S, et al. Damp heat stability and annealing behavior of aluminum doped zinc oxide films prepared by magnetron sputtering. *Thin Solid Films*. 2006;511-512:673-677. doi:[10.1016/j.tsf.2005.12.130](https://doi.org/10.1016/j.tsf.2005.12.130)
  88. Minami T, Kuboi T, Miyata T, Ohtani Y. Stability in a high humidity environment of TCO thin films deposited at low temperatures. *Phys Status Solidi Appl Mater Sci*. 2008;205(2):255-260. doi:[10.1002/pssa.200622541](https://doi.org/10.1002/pssa.200622541)
  89. Mei-Zhen G, Ke X, Fahrner WR. Study of the morphological change of amorphous ITO films after temperature-humidity treatment. *J Non Cryst Solids*. 2009;355(52-54):2682-2687. doi:[10.1016/j.jnoncrsol.2009.09.032](https://doi.org/10.1016/j.jnoncrsol.2009.09.032)
  90. Theelen M, Harel S, Verschuren M, et al. Influence of Mo/MoSe<sub>2</sub> microstructure on the damp heat stability of the Cu(In,Ga)Se<sub>2</sub> back contact molybdenum. *Thin Solid Films*. 2016;612:381-392. doi:[10.1016/j.tsf.2016.06.028](https://doi.org/10.1016/j.tsf.2016.06.028)
  91. Westin P, Neretnieks P, Edoff M. Damp heat degradation of CIGS-based PV modules. In *21st European Photovoltaic Solar Energy Conference*. IEEE; 2006:4-8.
  92. Klaer J, Klenk R, Boden A, et al. Damp heat stability of chalcopyrite mini-modules: evaluation of specific test structures. *Conf Rec IEEE Photovolt Spec Conf*; 2005:336-339. doi:[10.1109/pvsc.2005.1488137](https://doi.org/10.1109/pvsc.2005.1488137)
  93. Wennerberg J, Kessler J, Stolt L. Cu(In,Ga)Se-based thin-film photovoltaic modules optimized for long-term performance. *Sol Energy Mater Sol Cells*. 2003;75(1-2):47-55. doi:[10.1016/S0927-0248\(02\)00101-0](https://doi.org/10.1016/S0927-0248(02)00101-0)
  94. Theelen M, Hans V, Barreau N, Steijvers H, Vroon Z, Zeman M. The impact of alkali elements on the degradation of CIGS solar cells. *Prog Photovoltaics Res Appl*. 2015;23(5):537-545. doi:[10.1002/pip.2610](https://doi.org/10.1002/pip.2610)
  95. Theelen M, Hendrikx R, Barreau N, Steijvers H, Böttger A. The effect of damp heat-illumination exposure on CIGS solar cells: a combined XRD and electrical characterization study. *Sol Energy Mater Sol Cells*. 2016;157:943-952. doi:[10.1016/j.solmat.2016.07.051](https://doi.org/10.1016/j.solmat.2016.07.051)
  96. Yamaguchi S, Jonai S, Hara K, et al. Potential-induced degradation of Cu(In,Ga)Se<sub>2</sub> photovoltaic modules. *Jpn J Appl Phys*. 2015;54(8S1):08KC13. doi:[10.7567/JJAP.54.08KC13](https://doi.org/10.7567/JJAP.54.08KC13)
  97. Harvey SP, Guthrey H, Muzzillo CP, et al. Investigating PID shunting in polycrystalline CIGS devices via multi-scale. *IEEE J Photovoltaics*. 2019;9(2):559-564. doi:[10.1109/JPHOTOV.2019.2892874](https://doi.org/10.1109/JPHOTOV.2019.2892874)
  98. Fjallstrom V, Salome PMP, Hultqvist A, et al. Potential-induced degradation of CuIn<sub>1-x</sub>Ga<sub>x</sub>Se<sub>2</sub>.pdf. *IEEE J Photovoltaics*. 2013;3(3):1090-1094.
  99. Guillemoles JF. The puzzle of Cu(In,Ga)Se<sub>2</sub> (CIGS) solar cells stability. *Thin Solid Films*. 2002;403-404:405-409. doi:[10.1016/S0040-6090\(01\)01519-X](https://doi.org/10.1016/S0040-6090(01)01519-X)
  100. Bakker K, Ahman HN, Burgers T, Barreau N, Weeber A, Theelen M. Propagation mechanism of reverse bias induced defects in Cu(In,Ga)Se<sub>2</sub> solar cells. *Sol Energy Mater Sol Cells*. 2020;205:110249. doi:[10.1016/j.solmat.2019.110249](https://doi.org/10.1016/j.solmat.2019.110249)
  101. Westin P, Zimmerman U, Stolt L, Edoff M. Reverse bias damage in CIGS modules. In *IEEE PVSC*; 2009.
  102. Palmiotti E, Johnston S, Gerber A, et al. Identification and analysis of partial shading breakdown sites in CuIn<sub>x</sub>Ga(1-x)Se<sub>2</sub> modules. *Sol Energy*. 2018;161:1-5. doi:[10.1016/j.solener.2017.12.019](https://doi.org/10.1016/j.solener.2017.12.019)
  103. Silverman TJ, Deceglie MG, Deline C, Kurtz S. Partial shade stress test for thin-film photovoltaic modules. In: *Reliability of Photovoltaic Cells, Modules, Components, and Systems VIII*, vol. 9563 95630F. International Society for Optics and Photonics; 2015.
  104. Bakker K, Weeber A, Theelen M. Reliability implications of partial shading on CIGS photovoltaic devices: a literature review. *J Mater Res*. 2019;34(24):3977-3987. doi:[10.1557/jmr.2019.373](https://doi.org/10.1557/jmr.2019.373)
  105. Lany S, Zunger A. Light- and bias-induced metastabilities in Cu(In,Ga)Se<sub>2</sub> based solar cells caused by the (V<sub>Se</sub>-V<sub>Cu</sub>) vacancy complex. *J Appl Phys*. 2006;100(11):113725. doi:[10.1063/1.2388256](https://doi.org/10.1063/1.2388256)
  106. Mortazavi S, Bakker K, Carolus J, et al. Effect of reverse bias voltages on small scale gridded CIGS solar cells. In: *2017 IEEE 44th Photovoltaic Specialist Conference (PVSC)*. IEEE; 2017. <https://ieeexplore.ieee.org/abstract/document/8366514>
  107. Dongaonkar S, Alam MA. A shade tolerant panel design for thin film photovoltaics. *Conf. Rec. IEEE Photovolt. Spec. Conf.*; 2012: 2416-2420. doi:[10.1109/PVSC.2012.6318084](https://doi.org/10.1109/PVSC.2012.6318084)
  108. Silverman TJ, Mansfield L, Repins I, Kurtz S. Damage in monolithic thin-film photovoltaic modules due to partial shade. *IEEE J Photovoltaics*. 2016;6(5):1333-1338. doi:[10.1109/JPHOTOV.2016.2591330](https://doi.org/10.1109/JPHOTOV.2016.2591330)
  109. Puttnins S, Jander S, Pelz K, et al. The influence of front contact and buffer layer properties on CIGSe solar cell breakdown characteristics. *26th Eur Photovolt sol Energy Conf Exhib*; 2011: 2432-2434. doi:[10.4229/26thEUPVSEC2011-3CO.4.6](https://doi.org/10.4229/26thEUPVSEC2011-3CO.4.6)
  110. Silverman TJ, Mansfield L, Repins I, Kurtz S. Damage in monolithic thin-film photovoltaic modules due to partial shade. *2017 IEEE 44th Photovolt Spec Conf PVSC*. 2017;2017(6):1-6.
  111. Lee JE, Bae S, Oh W, et al. Investigation of damage caused by partial shading of CuIn<sub>x</sub>Ga(1-x)Se<sub>2</sub> photovoltaic modules with bypass diodes. *Prog Photovoltaics Res Appl*. 2016;24(8):1035-1043. doi:[10.1002/pip.2738](https://doi.org/10.1002/pip.2738)
  112. Espinosa N, García-Valverde R, Krebs FC. Life-cycle analysis of product integrated polymer solar cells. *Energy Environ Sci*. 2011;4(5):1547-1557. doi:[10.1039/c1ee01127h](https://doi.org/10.1039/c1ee01127h)
  113. O'regan B, Grätzel M. A low-cost, high-efficiency solar cell based on dye-sensitized colloidal TiO<sub>2</sub> films. *Nature*. 1991;353:737-740. doi:[10.1038/353737a0](https://doi.org/10.1038/353737a0)
  114. Li M, Igbari F, Wang ZK, Liao LS. Indoor thin-film photovoltaics: progress and challenges. *Adv Energy Mater*. 2020;10(28):2000641. doi:[10.1002/aenm.202000641](https://doi.org/10.1002/aenm.202000641)
  115. Freitag M, Teuscher J, Saygili Y, et al. Dye-sensitized solar cells for efficient power generation under ambient lighting. *Nat Photonics*. 2017;11(6):372-378. doi:[10.1038/nphoton.2017.60](https://doi.org/10.1038/nphoton.2017.60)
  116. Green MA, Dunlop ED, Hohl-Ebinger J, Yoshita M, Kopidakis N, Ho-Baillie AWY. Solar cell efficiency tables (Version 55). *Prog Photovoltaics Res Appl*. 2020;28(1):3-15. doi:[10.1002/pip.3228](https://doi.org/10.1002/pip.3228)
  117. Vlachopoulos N, Hagfeldt A. Photoelectrochemical cells based on dye sensitization for electricity and fuel production. *Chimia (Aarau)*. 2019;73(11):894-905. doi:[10.2533/chimia.2019.894](https://doi.org/10.2533/chimia.2019.894)
  118. Li G, Sheng L, Li T, Hu J, Li P, Wang K. Engineering flexible dye-sensitized solar cells for portable electronics. *Sol Energy*. 2019;177:80-98. doi:[10.1016/j.solener.2018.11.017](https://doi.org/10.1016/j.solener.2018.11.017)
  119. Hinsch A, Veurman W, Brandt H, Loayza Aguirre R, Bialecka K, Flarup Jensen K. Worldwide first fully up-scaled fabrication of 60 × 100 cm<sup>2</sup> dye solar module prototypes. *Prog Photovoltaics Res Appl*. 2012;20(6):698-710. doi:[10.1002/pip.1213](https://doi.org/10.1002/pip.1213)
  120. Park J, Lee P, Ko MJ. Design and fabrication of long-term stable dye-sensitized solar cells: effect of water contents in electrolytes on the performance. *Int J Precis Eng Manuf - Green Technol*. 2019;6(1):125-131. doi:[10.1007/s40684-019-00025-4](https://doi.org/10.1007/s40684-019-00025-4)
  121. Leandri V, Ellis H, Gabrielsson E, Sun L, Boschloo G, Hagfeldt A. An organic hydrophilic dye for water-based dye-sensitized solar cells. *Phys Chem Chem Phys*. 2014;16(37):19964-19971. doi:[10.1039/C4CP02774D](https://doi.org/10.1039/C4CP02774D)

122. Javaid R, Qazi UY. Catalytic oxidation process for the degradation of synthetic dyes: An overview. *Int J Environ Res Public Health*. 2019; 16(11):1-27. doi:10.3390/ijerph16112066
123. Yun S, Hagfeldt A. *Counter electrodes for dye-sensitized and perovskite solar cells*. Wiley-VCH Verlag GmbH & Co. KGaA; 2018. doi:10.1002/9783527813636
124. Iftikhar H, Sonai GG, Hashmi SG, Nogueira AF, Lund PD. Progress on electrolytes development in dye-sensitized solar cells. *Materials (Basel)*. 2019;12(12):1-68. doi:10.3390/ma12121998
125. Li CT, Lin RYY, Lin JT. Sensitizers for aqueous-based solar cells. *Chem - an Asian J*. 2017;12(5):486-496. doi:10.1002/asia.201601627
126. Bella F, Galliano S, Piana G, et al. Boosting the efficiency of aqueous solar cells: a photoelectrochemical estimation on the effectiveness of TiCl<sub>4</sub> treatment. *Electrochim Acta*. 2019;302:31-37. doi:10.1016/j.electacta.2019.01.180
127. Kakiage K, Aoyama Y, Yano T, Oya K, Fujisawa JI, Hanaya M. Highly-efficient dye-sensitized solar cells with collaborative sensitization by silyl-anchor and carboxy-anchor dyes. *Chem Commun*. 2015;51(88):15894-15897. doi:10.1039/C5CC06759F
128. Bella F, Galliano S, Gerbaldi C, Viscardi G. Cobalt-based electrolytes for dye-sensitized solar cells: Recent advances towards stable devices. *Energies*. 2016;9(5):1-22. doi:10.3390/en9050384
129. Hu M, Shen J, Yu Z, et al. Efficient and stable dye-sensitized solar cells based on a tetradentate copper (II/I) redox mediator. *ACS Appl Mater Interfaces*. 2018;10(36):30409-30416. doi:10.1021/acsami.8b10182
130. Hashmi G, Miettunen K, Peltola T, et al. Review of materials and manufacturing options for large area flexible dye solar cells. *Renew Sustain Energy Rev*. 2011;15(8):3717-3732. doi:10.1016/j.rser.2011.06.004
131. Tiihonen A, Miettunen K, Halme J, Lepikko S, Poskela A, Lund PD. Critical analysis on the quality of stability studies of perovskite and dye solar cells. *Energ Environ Sci*. 2018;11(4):730-738. doi:10.1039/C7EE02670F
132. Smestad GP, Krebs FC, Lampert CM, et al. Reporting solar cell efficiencies in solar energy materials and solar cells. *Sol Energy Mater Sol Cells*. 2008;92(4):371-373. doi:10.1016/j.solmat.2008.01.003
133. Espinosa N, García-Valverde R, Urbina A, et al. Life cycle assessment of ITO-free flexible polymer solar cells prepared by roll-to-roll coating and printing. *Sol Energy Mater Sol Cells*. 2012;97:3-13. doi:10.1016/j.solmat.2011.09.048
134. Azzopardi B, Emmott CJM, Urbina A, Krebs FC, Mutale J, Nelson J. Economic assessment of solar electricity production from organic-based photovoltaic modules in a domestic environment. *Energ Environ Sci*. 2011;4(10):3741-3753. doi:10.1039/c1ee01766g
135. Cui Y, Yao H, Zhang J, et al. Over 16% efficiency organic photovoltaic cells enabled by a chlorinated acceptor with increased open-circuit voltages. *Nat Commun*. 2019;10(1):1-8. doi:10.1038/s41467-019-10351-5
136. Ma L-K, Chen Y, Chow PCY, et al. High-efficiency indoor organic photovoltaics with a band-aligned interlayer. *Aust Dent J*. 2020;4(7):1486-1500. doi:10.1016/j.joule.2020.05.010
137. Reese MO, Gevorgyan SA, Jørgensen M, et al. Consensus stability testing protocols for organic photovoltaic materials and devices. *Sol Energy Mater Sol Cells*. 2011;95(5):1253-1267. doi:10.1016/j.solmat.2011.01.036
138. Ye M, Chen C, Zhang N, Wen X, Guo W, Lin C. Quantum-dot sensitized solar cells employing hierarchical Cu<sub>2</sub>S microspheres wrapped by reduced graphene oxide nanosheets as effective counter electrodes. *Adv Energy Mater*. 2014;4(9):1301564. doi:10.1002/aenm.201301564
139. Mateker WR, McGehee MD. Progress in understanding degradation mechanisms and improving stability in organic photovoltaics. *Adv Mater*. 2017;29(10):1603940. doi:10.1002/adma.201603940
140. Kettle J, Bristow N, Gethin DT, et al. Printable luminescent down shifter for enhancing efficiency and stability of organic photovoltaics. *Sol Energy Mater Sol Cells*. 2016;144:481-487. doi:10.1016/j.solmat.2015.09.037
141. Kettle J, Bristow N, Sweet TKN, et al. Three dimensional corrugated organic photovoltaics for building integration; improving the efficiency, oblique angle and diffuse performance of solar cells. *Energ Environ Sci*. 2015;8(11):3266-3273. doi:10.1039/C5EE02162F
142. Cheng P, Zhan X. Stability of organic solar cells: challenges and strategies. *Chem Soc Rev*. 2016;45(9):2544-2582. doi:10.1039/C5CS00593K
143. Gevorgyan SA, Heckler IM, Bundgaard E, et al. Improving, characterizing and predicting the lifetime of organic photovoltaics. *J Phys D Appl Phys*. 2017;50(10):103001. doi:10.1088/1361-6463/50/10/103001
144. Corazza M, Krebs FC, Gevorgyan SA. Predicting, categorizing and intercomparing the lifetime of OPVs for different ageing tests. *Sol Energy Mater Sol Cells*. 2014;130:99-106. doi:10.1016/j.solmat.2014.06.031
145. Stoichkov V, Kumar D, Tyagi P, Kettle J. Multistress testing of OPV modules for accurate predictive aging and reliability predictions. *IEEE J Photovoltaics*. 2018;8(4):1058-1065. doi:10.1109/JPHOTOV.2018.2838438
146. Kettle J, Acobsson J. *Enhancing the stability of Organic Photovoltaics through Machine Learning*. Nano Energy, Elsevier; 2020. doi:10.1016/j.nanoen.2020.105342
147. Odabaşı Ç, Yıldırım R. Performance analysis of perovskite solar cells in 2013–2018 using machine-learning tools. *Nano Energy*. 2019;56:770-791. doi:10.1016/j.nanoen.2018.11.069
148. David TW, Anizelli H, Tyagi P, Gray C, Teahan W, Kettle J. Using large datasets of organic photovoltaic performance data to elucidate trends in reliability between 2009 and 2019. *IEEE J Photovoltaics*. 2019;9(6):1768-1773. doi:10.1109/JPHOTOV.2019.2939070
149. Baran D, Ashraf RS, Hanifi DA, et al. Reducing the efficiency–stability–cost gap of organic photovoltaics with highly efficient and stable small molecule acceptor ternary solar cells. *Nat Mater*. 2017;16(3):363-369. doi:10.1038/nmat4797
150. Du X, Heumueller T, Gruber W, et al. Efficient polymer solar cells based on non-fullerene acceptors with potential device lifetime approaching 10 years. *Aust Dent J*. 2019;3(1):215-226. doi:10.1016/j.joule.2018.09.001
151. Bristow N, Kettle J. Outdoor performance of organic photovoltaics: diurnal analysis, dependence on temperature, irradiance, and degradation. *J Renew Sustain Energy*. 2015;7(1):13111. doi:10.1063/1.4906915
152. Zhang Y, Samuel IDW, Wang T, Lidzey DG. Current status of outdoor lifetime testing of organic photovoltaics. *Adv Sci*. 2018;5(8):1800434. doi:10.1002/adv.201800434
153. Soares GA, David TW, Anizelli H, et al. Outdoor performance of organic photovoltaics at two different locations: a comparison of degradation and the effect of condensation. *J Renew Sustain Energy*. 2020;12(6):63502. doi:10.1063/5.0025622
154. Katz EA, Gevorgyan S, Orynbayev MS, Krebs FC. Out-door testing and long-term stability of plastic solar cells. *Eur Phys Journal-Applied Phys*. 2006;36(3):307-311. doi:10.1051/epjap:2006159
155. Josey DS, Nyikos SR, Garner RK, et al. Outdoor performance and stability of boron subphthalocyanines applied as electron acceptors in fullerene-free organic photovoltaics. *ACS Energy Lett*. 2017;2(3):726-732. doi:10.1021/acsenerylett.6b00716
156. Garner RK, Josey DS, Nyikos SR, et al. Boron subphthalocyanines as electron donors in outdoor lifetime monitored organic photovoltaic cells. *Sol Energy Mater Sol Cells*. 2018;176:331-335. doi:10.1016/j.solmat.2017.10.018
157. Krebs FC, Espinosa N, Hösel M, Søndergaard RR, Jørgensen M. 25th anniversary article: rise to power—OPV-based solar parks. *Adv Mater*. 2014;26(1):29-39. doi:10.1002/adma.201302031

158. Kazim S, Nazeeruddin MK, Grätzel M, Ahmad S. Perovskite as light harvester: a game changer in photovoltaics. *Angew Chem Int Ed*. 2014;53(11):2812-2824. doi:10.1002/anie.201308719
159. Kojima A, Teshima K, Shirai Y, Miyasaka T. Organometal halide perovskites as visible-light sensitizers for photovoltaic cells. *J Am Chem Soc*. 2009;131(17):6050-6051. doi:10.1021/ja809598r
160. Green MA, Dunlop E, Hohl-Ebinger J, Yoshita M, Kopidakis N, Hao X. Solar cell efficiency tables (Version 57). *Prog Photovoltaics Res Appl*. 2021;29(1):3-15. doi:10.1002/PIP.3371
161. NREL. Best research-cell efficiency chart. <https://www.nrel.gov/pv/cell-efficiency.html>
162. Al-Ashouri A, Köhnen E, Li B, et al. Monolithic perovskite/silicon tandem solar cell with > 29% efficiency by enhanced hole extraction. *Science*. 2020;370(6522):1300-1309. doi:10.1126/science.abd4016
163. Lee MM, Teuscher J, Miyasaka T, Murakami TN, Snaith HJ. Efficient hybrid solar cells based on meso-superstructured organometal halide perovskites. *Science*. 2012;338(6107):643-647. doi:10.1126/science.1228604
164. Kim H-S, Lee CR, Im JH, et al. Lead iodide perovskite sensitized all-solid-state submicron thin film mesoscopic solar cell with efficiency exceeding 9%. *Sci Rep*. 2012;2(1):591. doi:10.1038/srep00591
165. Lin R, Xu J, Wei M, et al. All-perovskite tandem solar cells with improved grain surface passivation. *Nature*. 2022;603:73-78. doi:10.1038/s41586-021-04372-8
166. Kapil G, Bessho T, Maekawa T, et al. Tin-lead perovskite fabricated via ethylenediamine interlayer guides to the solar cell efficiency of 21.74%. *Adv Energy Mater*. 2021;11(25):2101069. doi:10.1002/aenm.202101069
167. Xiao K, Lin R, Han Q, et al. All-perovskite tandem solar cells with 24.2% certified efficiency and area over 1 cm<sup>2</sup> using surface-anchoring zwitterionic antioxidant. *Nat Energy*. 2020;5(11):870-880. doi:10.1038/s41560-020-00705-5
168. Perovskite database. 2020. [www.perovskitedatabase.com](http://www.perovskitedatabase.com)
169. Salado M, Kazim S, Ahmad S. The role of Cs<sup>+</sup> inclusion in formamidinium lead triiodide-based perovskite solar cell. *Chem Pap*. 2018;72(7):1645-1650. doi:10.1007/s11696-017-0373-7
170. Salado M, Calio L, Berger R, Kazim S, Ahmad S. Influence of the mixed organic cation ratio in lead iodide based perovskite on the performance of solar cells. *Phys Chem Chem Phys*. 2016;18:27148-27157. doi:10.1039/c6cp03851d
171. Salado M, Shirzadi E, Kazim S, et al. Oxazolium Iodide Modified Perovskites for Solar Cell Fabrication. *ChemPlusChem*. 2018;83(4):279-284. doi:10.1002/cplu.201700471
172. Salado M, Kazim S, Nazeeruddin MK, Ahmad S. Appraisal of crystal expansion in CH<sub>3</sub>NH<sub>3</sub>PbI<sub>3</sub> on doping: improved photovoltaic properties. *ChemSusChem*. 2019;12:2366-2372. doi:10.1002/cssc.201803043
173. Shin SS, Yeom EJ, Yang WS, et al. Colloidally prepared La-doped BaSnO<sub>3</sub> electrodes for efficient, photostable perovskite solar cells. *Science*. 2017;356(6334):167-171. doi:10.1126/science.aam6620
174. Zhang H, Wang H, Chen W, Jen AKY. CuGaO<sub>2</sub>: a promising inorganic hole-transporting material for highly efficient and stable perovskite solar cells. *Adv Mater*. 2017;29(8):1604984. doi:10.1002/adma.201604984
175. Stolterfoht M, Wolff CM, Amir Y, et al. Approaching the fill factor Shockley-Queisser limit in stable, dopant-free triple cation perovskite solar cells. *Energy Environ Sci*. 2017;10(6):1530-1539. doi:10.1039/C7EE00899F
176. Anizelli H, David TW, Tyagi P, Laureto E, Kettle J. Enhancing the stability of perovskite solar cells through functionalisation of metal oxide transport layers with self-assembled monolayers. *Sol Energy*. 2020;203:157-163. doi:10.1016/j.solener.2020.04.035
177. Rong Y, Hu Y, Mei A, et al. Challenges for commercializing perovskite solar cells. *Science*. 2018;361(6408):eaat8235. doi:10.1126/science.aat8235
178. Wei Y, Li W, Xiang S, et al. Precursor effects on methylamine gas-induced CH<sub>3</sub>NH<sub>3</sub>PbI<sub>3</sub> films for stable carbon-based perovskite solar cells. *Sol Energy*. 2018;174:139-148. doi:10.1016/j.solener.2018.09.003
179. Li Y, Xu X, Wang C, et al. Light-induced degradation of CH<sub>3</sub>NH<sub>3</sub>PbI<sub>3</sub> hybrid perovskite thin film. *J Phys Chem C*. 2017;121(7):3904-3910. doi:10.1021/acs.jpcc.6b11853
180. Bryant D, Aristidou N, Pont S, et al. Light and oxygen induced degradation limits the operational stability of methylammonium lead triiodide perovskite solar cells. *Energy Environ Sci*. 2016;9(5):1655-1660. doi:10.1039/C6EE00409A
181. Chi W, Banerjee SK. Stability improvement of perovskite solar cells by compositional and interfacial engineering. *Chem Mater*. 2021;33(5):1540-1570. doi:10.1021/acs.chemmater.0c04931
182. Khenkin MV, Katz EA, Abate A, et al. Consensus statement for stability assessment and reporting for perovskite photovoltaics based on ISOS procedures. *Nat Energy*. 2020;5(1):35-49. doi:10.1038/s41560-019-0529-5
183. Ito S, Tanaka S, Manabe K, Nishino H. Effects of surface blocking layer of Sb<sub>2</sub>S<sub>3</sub> on nanocrystalline TiO<sub>2</sub> for CH<sub>3</sub>NH<sub>3</sub>PbI<sub>3</sub> perovskite solar cells. *J Phys Chem C*. 2014;118(30):16995-17000. doi:10.1021/jp500449z
184. Misra RK, Aharon S, Li B, et al. Temperature- and component-dependent degradation of perovskite photovoltaic materials under concentrated sunlight. *J Phys Chem Lett*. 2015;6(3):326-330. doi:10.1021/jz502642b
185. Aristidou N, Sanchez-Molina I, Chotchuangchuchaval T, et al. The role of oxygen in the degradation of methylammonium lead trihalide perovskite photoactive layers. *Angew Chem Int Ed*. 2015;54(28):8208-8212. doi:10.1002/anie.201503153
186. Lee S-W, Kim S, Bae S, et al. UV degradation and recovery of perovskite solar cells. *Sci Rep*. 2016;6(1):38150. doi:10.1038/srep38150
187. Liu R, Wang L, Fan Y, Li Z, Pang S. UV degradation of the interface between perovskites and the electron transport layer. *RSC Adv*. 2020;10(20):11551-11556. doi:10.1039/C9RA10960A
188. Moslah C, Mousdis GA, Kandyala M, Petropoulou G, Ksibi M. Photocatalytic Properties of TiO<sub>2</sub> Thin Films Doped With Noble Metals (Ag, Au, Pd and Pt) for Water Decontamination. In: Bonča J, Kruchinin S, eds. *Nanostructured Materials for the Detection of CBRN*. NATO Science for Peace and Security Series A: Chemistry and Biology. Springer, Dordrecht; 2018. doi:10.1007/978-94-024-1304-5\_6
189. Niu G, Guo X, Wang L. Review of recent progress in chemical stability of perovskite solar cells. *J Mater Chem A*. 2015;3(17):8970-8980. doi:10.1039/C4TA04994B
190. Ji J, Liu X, Jiang H, et al. Two-stage ultraviolet degradation of perovskite solar cells induced by the oxygen vacancy-Ti<sup>4+</sup> states. *iScience*. 2020;23(4):101013. doi:10.1016/j.isci.2020.101013
191. Kwak K, Lim E, Ahn N, et al. An atomistic mechanism for the degradation of perovskite solar cells by trapped charge. *Nanoscale*. 2019;11(23):11369-11378. doi:10.1039/C9NR02193K
192. Christians JA, Miranda Herrera PA, Kamat PV. Transformation of the excited state and photovoltaic efficiency of CH<sub>3</sub>NH<sub>3</sub>PbI<sub>3</sub> perovskite upon controlled exposure to humidified air. *J Am Chem Soc*. 2015;137(4):1530-1538. doi:10.1021/ja511132a
193. Schoonman J. Organic-inorganic lead halide perovskite solar cell materials: a possible stability problem. *Chem Phys Lett*. 2015;619:193-195. doi:10.1016/j.cplett.2014.11.063
194. Leijtens T, Eperon GE, Pathak S, Abate A, Lee MM, Snaith HJ. Overcoming ultraviolet light instability of sensitized TiO<sub>2</sub> with meso-superstructured organometal tri-halide perovskite solar cells. *Nat Commun*. 2013;4(1):2885. doi:10.1038/ncomms3885
195. Checharoen R, Bush KA, Rolston N, et al. Damp heat, temperature cycling and uv stress testing of encapsulated perovskite photovoltaic cells. 2018 IEEE 7th World Conf. Photovolt. Energy Conversion,

- WCPEC 2018 - A Jt. Conf. 45th IEEE PVSC, 28th PVSEC 34th EU PVSEC 1; 2018:3498-;3502.
196. Spectrum-Dependent Spiro-OMeTAD oxidization mechanism in perovskite solar cells; 2015. doi:[10.1021/acsami.5b07703](https://doi.org/10.1021/acsami.5b07703).
  197. Wei D, Wang T, Ji J, et al. Photo-induced degradation of lead halide perovskite solar cells caused by the hole transport layer/metal electrode interface. *J Mater Chem A*. 2016;4(5):1991-1998. doi:[10.1039/C5TA08622A](https://doi.org/10.1039/C5TA08622A)
  198. Lee JW, Kim DH, Kim HS, Seo SW, Cho SM, Park NG. Formamidinium and cesium hybridization for photo- and moisture-stable perovskite solar cell. *Adv Energy Mater*. 2015;5(20):1501310. doi:[10.1002/aenm.201501310](https://doi.org/10.1002/aenm.201501310)
  199. Haris MPU, Kazim S, Pegu M, Deepa M, Ahmad S. Substance and Shadow of Formamidinium Lead Triiodide Based Solar Cells. *Phys Chem Chem Phys*. 2021;23(15):9049-9060. doi:[10.1039/D1CP00552A](https://doi.org/10.1039/D1CP00552A)
  200. Kumar A, Bansode U, Ogale S, Rahman A. Understanding the thermal degradation mechanism of perovskite solar cells via dielectric and noise measurements. *Nanotechnology*. 2020;31(36):365403. doi:[10.1088/1361-6528/ab97d4](https://doi.org/10.1088/1361-6528/ab97d4)
  201. Akbulatov AF, Tsarev SA, Elshobaki M, et al. Comparative intrinsic thermal and photochemical stability of Sn (II) complex halides as next-generation materials for lead-free perovskite solar cells. *J Phys Chem C*. 2019;123(44):26862-26869. doi:[10.1021/acs.jpcc.9b09200](https://doi.org/10.1021/acs.jpcc.9b09200)
  202. Divitini G, Cavovich S, Matteocci F, Cinà L, di Carlo A, Ducati C. In situ observation of heat-induced degradation of perovskite solar cells. *Nat Energy*. 2016;1(2):15012. doi:[10.1038/nenergy.2015.12](https://doi.org/10.1038/nenergy.2015.12)
  203. Dualeh A, Gao P, Seok SI, Nazeeruddin MK, Grätzel M. Thermal behavior of methylammonium lead-trihalide perovskite photovoltaic light harvesters. *Chem Mater*. 2014;26(21):6160-6164. doi:[10.1021/cm502468k](https://doi.org/10.1021/cm502468k)
  204. Kim NK, Min YH, Noh S, et al. Investigation of thermally induced degradation in CH<sub>3</sub>NH<sub>3</sub>PbI<sub>3</sub> perovskite solar cells using in-situ synchrotron radiation analysis. *Sci Rep*. 2017;7:1-9. doi:[10.1038/s41598-017-04690-w](https://doi.org/10.1038/s41598-017-04690-w)
  205. Juarez-Perez EJ, Hawash Z, Raga SR, Ono LK, Qi Y. Thermal degradation of CH<sub>3</sub>NH<sub>3</sub>PbI<sub>3</sub> perovskite into NH<sub>3</sub> and CH<sub>3</sub>I gases observed by coupled thermogravimetry-mass spectrometry analysis. *Energy Environ Sci*. 2016;9(11):3406-3410. doi:[10.1039/C6EE02016J](https://doi.org/10.1039/C6EE02016J)
  206. Domanski K, Correa-Baena JP, Mine N, et al. Not all that glitters is gold: metal-migration-induced degradation in perovskite solar cells. *ACS Nano*. 2016;10(6):6306-6314. doi:[10.1021/acsnano.6b02613](https://doi.org/10.1021/acsnano.6b02613)
  207. Jena AK, Ikegami M, Miyasaka T. severe morphological deformation of Spiro-OMeTAD in (CH<sub>3</sub>NH<sub>3</sub>)PbI<sub>3</sub> solar cells at high temperature. *ACS Energy Lett*. 2017;2(8):1760-1761. doi:[10.1021/acsenerylett.7b00582](https://doi.org/10.1021/acsenerylett.7b00582)
  208. Rolston N, Printz AD, Tracy JM, et al. Effect of cation composition on the mechanical stability of perovskite solar Cells. *Adv Energy Mater*. 2018;8:1-7. doi:[10.1002/aenm.201702116](https://doi.org/10.1002/aenm.201702116)
  209. Kettle J, Waters H, Ding Z, Horie M, Smith GC. Chemical changes in PCPDTBT: PCBM solar cells using XPS and TOF-SIMS and use of inverted device structure for improving lifetime performance. *Sol Energy Mater Sol Cells*. 2015;141:139-147. doi:[10.1016/j.solmat.2015.05.016](https://doi.org/10.1016/j.solmat.2015.05.016)
  210. Rolston N, Watson BL, Bailie CD, et al. Mechanical integrity of solution-processed perovskite solar cells. *Extrem Mech Lett*. 2016;9:353-358. doi:[10.1016/j.eml.2016.06.006](https://doi.org/10.1016/j.eml.2016.06.006)
  211. Li Y, Meng L, Yang YM, et al. High-efficiency robust perovskite solar cells on ultrathin flexible substrates. *Nat Commun*. 2016;7:10214. doi:[10.1038/ncomms10214](https://doi.org/10.1038/ncomms10214)
  212. Guarnera S, Abate A, Zhang W, et al. Improving the long-term stability of perovskite solar cells with a porous Al<sub>2</sub>O<sub>3</sub> buffer layer. *J Phys Chem Lett*. 2015;6(3):432-437. doi:[10.1021/jz502703p](https://doi.org/10.1021/jz502703p)
  213. Davis A, Tran T, Young DR. Solution chemistry of iodide leaching of gold. *Hydrometallurgy*. 1993;32(2):143-159. doi:[10.1016/0304-386X\(93\)90020-E](https://doi.org/10.1016/0304-386X(93)90020-E)
  214. Jeong M, Choi IW, Go EM, et al. Stable perovskite solar cells with efficiency exceeding 24.8% and 0.3-V voltage loss. *Science*. 2020;369(6511):1615-1620. doi:[10.1126/science.abb7167](https://doi.org/10.1126/science.abb7167)

**How to cite this article:** Kettle J, Aghaei M, Ahmad S, et al. Review of technology specific degradation in crystalline silicon, cadmium telluride, copper indium gallium selenide, dye sensitised, organic and perovskite solar cells in photovoltaic modules: Understanding how reliability improvements in mature technologies can enhance emerging technologies. *Prog Photovolt Res Appl*. 2022;30(12):1365-1392. doi:[10.1002/pip.3577](https://doi.org/10.1002/pip.3577)